UNIVERSITAT POLITÈCNICA DE VALÈNCIA

TELECOM ESCUELA TÉCNICA VLC SUPERIOR DE UPV INGENIEROS DE TELECOMUNICACIÓN

Optimized design of planar microwave filters based on aggressive space mapping techniques

Author: Emilio Molina Tercero

Supervisor: Dr. Jorge Daniel Martínez Pérez

A Thesis in the Field of Microwave Filters for the Degree of Telecommunications Technologies and Services Engineering.
Escuela Técnica Superior de Ingenieros de Telecomunicación de la Universitat Politècnica de València

Year 2018-19

Valencia, September 10, 2019

Escuela Técnica Superior de Ingeniería de Telecomunicación
Universitat Politècnica de València
Edificio 4D. Camino de Vera, s/n, 46022 Valencia
Tel. +34 96 387 71 90, ext. 77190
www.etsit.upv.es

VLC/ CAMPUS VALENCIA, INTERNATIONAL CAMPUS OF EXCELLENCE

EMAS Gestión ambiental verificada

Acknowledgments

At the very outset of this report, I would like to express my sincere and heartfelt gratefulness to my parents for their moral encouragement. In addition, I must thank all my family and friends, specially Cristina and Alberto, for their unconditional help and support. Finally, I want to remark my gratitude to my supervisor Jorge Daniel Martínez Pérez and to the iTEAM members for all their trust and guidance through this challenging project.

Abstract

The use of aggressive space mapping algorithms (ASM) has aroused a growing interest in the field of design and optimization of microwave filters. This technique allows to minimize the number of EM simulations necessary to obtain the appropriate values for the geometric parameters of the structure that allows us to obtain a desired objective response. In this report, we intend to address the implementation of an ASM algorithm for the optimized design of planar filters with advanced responses (e.g. incorporating transmission zeros). One of the most important challenges is to ensure adequate parameter extraction of the coarse model from the EM simulation. This is especially relevant in the case of structures with significant loss levels or where concentrated models do not accurately model the actual behavior of the structure. The objective of this TFG is to analyze different optimization methods to perform the parameter extraction process as well as to evaluate the convergence of the method through its application to the design of narrow-band planar microwave filters with pseudo-elliptical and Chebyshev responses.

Resumen

El uso de algoritmos de mapeo espacial agresivo (Aggresive Space Mapping, ASM) ha despertado un creciente interés en el ámbito del diseño y la optimización de filtros de microondas. Esta técnica permite minimizar el número de simulaciones EM necesarias para obtener los valores adecuados de los parámetros geométricos de la estructura que permiten obtener una determinada respuesta objetivo. En el presente trabajo se pretende abordar la implementación de un algoritmo de ASM para el diseño optimizado de filtros planares con respuestas avanzadas (e.g. incorporando ceros de transmisión). Uno de los retos más importantes consiste en garantizar una extracción adecuada del modelo grueso a partir de la simulación EM. Esto es especialmente relevante en el caso de estructuras con niveles de pérdidas significativos o donde los modelos concentrados no modelan con precisión el comportamiento real de la estructura. El objetivo del TFG es analizar diferentes métodos de optimización para realizar el proceso de extracción paramétrica así como evaluar la convergencia del método mediante su aplicación al diseño de filtros de microondas planares de banda estrecha con respuestas pseudo-elíptica y Chebyshev.

Resum

L'ús d'algoritmes de mapatge espacial agressiu (Aggresive Space Mapping, ASM) ha despertat un creixent interés en l'àmbit del disseny i l'optimització de filtres de microones. Aquesta tècnica permet minimitzar el nombre de simulacions EM necessàries per a obtindre els valors adequats dels paràmetres geomètrics de l'estructura que permeten obtindre una determinada resposta objectiu. En el present treball es pretén abordar la implementació d'un algorisme de ASM per al disseny optimitzat de filtres planars amb respostes avançades (e.g. incorporant zeros de transmissió). Un dels reptes més importants consisteix a garantir una extracció adequada del model gruixut a partir de la simulació EM. Això és especialment rellevant en el cas d'estructures amb nivells de pèrdues significatives o on els models concentrats no modelen amb precisió el comportament real de l'estructura. L'objectiu del TFG és analitzar diferents mètodes d'optimització per a realitzar el procés d'extracció paramètrica així com avaluar la convergència del mètode mitjançant la seua aplicació al disseny de filtres de microones planars de banda estreta amb respostes pseudo-ellíptica i Chebyshev.

Contents

List of Figures

List of Tables

List of Abbreviations

ASM	Aggressive Space Mapping
EM	Electro-Magnetic
PE	Parameter Extraction
RF	Radio Frequency
TFG	End of Bachelor Degree Thesis
iTEAM	Institute of Telecommunications and Multimedia Applications

Chapter 1

Introduction, Objectives and Methodology

1.1 Overview

Born in the early 90's, the oldest forms of electronic filters are passive analog linear filters, implemented using just resistors R, inductors L, and capacitors C. The problem with those filters is that they are monopole filters, so their applications are very limited. These are known as RC and RL filters.

Multipole LC filters improve this issue, and provide greater control over the frequency response, bandwidth and transition bands. The first of these filters was invented by George Campbell in 1910, and it is known as the k-type filter. Together with other improved filters, these filters are known as image parameter filters.

A big step forward was taken by Cauer who was the founder of network synthesis around the time of World War II. Cauer's theory allowed filters to be constructed so that their frequency response followed some particular frequency function.

Simultaneously, microwave filters were being developed as well, but it was on the early 1960s, where the telecommunications field saw the rise of two more major development areas, microwave integrated circuits and solid-state microwave beginnings.

With the development of satellite communications, microwave relay stations, and the added growing in commercial and military radio detection and ranging, microwave engineering became a billion-dollar industry.

Nowadays, RF and microwave filter design is one of the main areas of research to provide solutions for the incoming challenges such as 5G implementation and what is yet to come.

1.2 Objectives

In this report, it will be studied how to optimize and implement microwave filters applying ASM algorithms, and also, it will be analyzed how to obtain an optimum performance of the algorithm itself.

To achieve this, a rigorous study about ASM technique applied to different filter topologies has been realized. The main purpose of this study, is to prove whether the application of the ASM technique is valid for various scenarios, which makes it a really powerful tool then, since we would be able to follow a more strict optimization process than compared to the traditional one, which is mainly based on the experience of the designer itself.
The main aspects which are going to be considered to evaluate the algorithm are the evolution of the parameters through the ASM iterations and of course, the resultant frequency response of the filter, as well as its convergence.

1.3 Project management

The report can be split into three clearly differentiated parts.
The first one corresponds to the theoretical study and understanding about RF and microwave filters. It is crucial to have a solid basis about how to design a filter given certain design conditions. Once the theoretical part about filter design is clear, its also important to study the Microstrip technology, how does it work, its advantages, and how to obtain our microstrip filter model derived from the theoretical one. This first part is probably one of the most important, since it is the one that will allow us to fully understand what we are trying to obtain applying ASM techniques, and furthermore, the whole aim of the report. This phase corresponds to Chap. 2.

The second part of the thesis consist on understanding and analyzing ASM. It is important to determine how does the algorithm behaves, how does it compensate the cross coupling effects present on the more compact structures and so on. In addition, this part involved the development of a Python script, able to compute all the required parameters of each ASM iteration, and save all the data into *.txt* files. This can be found in Chap. 3.

Finally, the last but not least important part is the filter designing one. In order to achieve this, Microwave Office AWR software was used, which allows us to design and simulate our filters and models. A similar frequency response Bandpass filter has been designed adopting two different topologies, as described in Chaps. 4 and 5.

To conclude, all the different achievements will be shown and we will briefly go over the future research lines in Chap. 6

1.4 Tasks Schedule

The tasks that have taken part in the development of this report are the following:

1. Research reading and understanding of various scientific articles, books and other reports.
2. Theoretical study about RF and microwave filter design and more specifically, about Chebyshev and pseudo-elliptical bandpass filters.
3. Study about microstrip technology, its basic concepts and learning how to implement filters using microstrip distributed elements.
4. Deeply understanding how to properly use the software tool used to carry out the design and simulation of the filters. In this case, AWR Microwave Office was chosen to perform all the needed simulations.
5. Study and research about ASM techniques and how to best implement.
   (a) Development of a Python Script to compute all the ASM iterations parameters.
6. Design of both bandpass filters
   (a) Theoretical model design to obtain the ideal response of the filter.
   (b) Microstrip filter model design.
   (c) Characterization of all the different filter curves needed to build the Broyden matrix B.
   (d) Starting point chosen, physical dimensions for the microstrip model filter set up and application of the ASM algorithm.
   (e) Simulations and results.
7. Conclusions and future research lines.
8. Report writing using LaTeX.

Chapter 2

RF and Microwave Filters Fundamentals

2.1 Introduction

Microwaves can be defined as those electromagnetic waves ranging from 300 MHz - 300 GHz. The characteristic wavelength of this waves ranges between 1 m - 1 mm. The electromagnetic spectrum can be seen in Fig. 2.1. Despite this definition, the boundaries of itself vary depending on the technology used for an specific application. The vast majority of these applications belong to the communications field, even though there are many more applications in these frequency ranges such as sensing, heating or imaging among others.

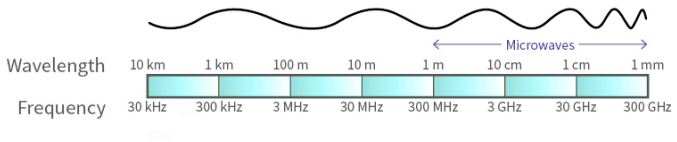

Figure 2.1: Electromagnetic spectrum.

2.2 RF Filters

As previously stated, there are millions of applications and devices using those frequency ranges. This fact raises the need of some device capable of isolating the particular spectrum we are interested at, so that we can get our useful information or data, and operate with it.
And right there, it is where filters stand out. RF and microwave filters have a fundamental role in communications systems and in any RF or microwave application, since they are in charge of rejecting or not certain frequency bands, along with many other utilities. There are several types of filters and

they can be classified in many ways. According to their effective or pass bands the main types are:

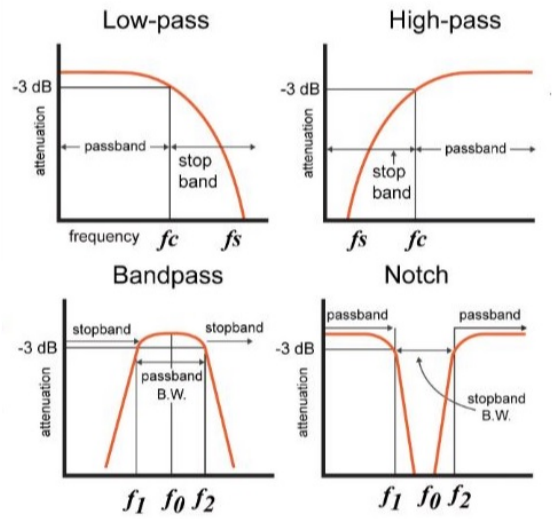

Figure 2.2: Frequency response of the main filter types. [14]

Taking into account the filter selectivity, ripple level in band and other parameters, we can distinguish between the following main filter responses:

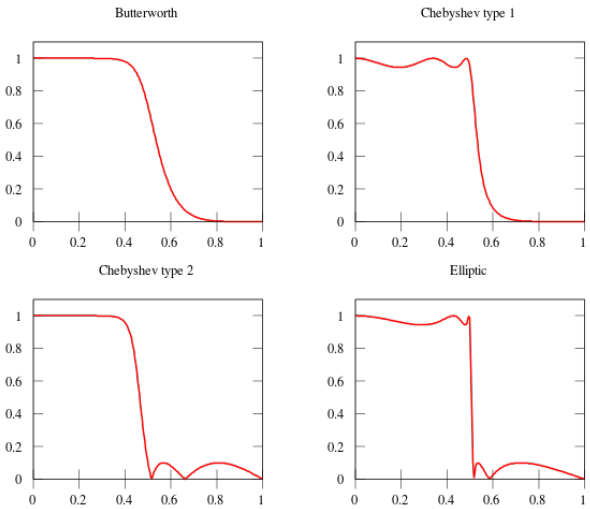

Figure 2.3: Classification in term of specs. [15]

The reason why Chebyshev and pseudo-elliptical bandpass filters are the most eligible type of filters for this project is because they have an average behavior, they are quite sharp filters, presenting great selectivity outside the pass band, and they are capable of dealing with ripple in the band as well, concentrating the error along the whole band in the most optimum way.

In addition, they are widely known and hundreds of designs and examples are available, which we

can refer to in order to test ASM techniques.

2.2.1 Scattering Parameters

The scattering parameters describe the electrical behavior of linear electrical networks.

In our case, since we are designing filters, we are going to consider two port networks.

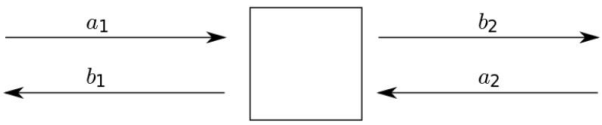

Figure 2.4: Two port network

And the relationship between input and output signals is given by:

$$\begin{bmatrix} b_1 \\ b_2 \end{bmatrix} = \begin{bmatrix} S_{11} & S_{12} \\ S_{21} & S_{22} \end{bmatrix} \times \begin{bmatrix} a_1 \\ a_2 \end{bmatrix}$$

Where S_{11} and S_{21} which are the return and transmission losses, can be obtained as:

$$S_{11} = \frac{b_1}{a_1} = \frac{V_1^-}{V_1^+}, \qquad S_{21} = \frac{b_2}{a_1} = \frac{V_2^-}{V_1^+} \tag{2.1}$$

These parameters are the main characterizes of filter frequency responses, and will be present along this report.

2.2.2 Chebyshev and Elliptical transfer functions

An ideal passive filter is a loss-less network with two accesses, whose transfer function is the mathematical expression for the scattering parameter S_{21}.

That function general form is:

$$|S_{21}(j\Omega)|^2 = \frac{1}{1 + \epsilon^2 F_n^2(\Omega)} \tag{2.2}$$

Where ϵ is the ripple constant and F_n the characteristic function.

Insertion and return losses L_A and L_R can be obtained from:

$$L_A(\Omega) = 10\ log\frac{1}{|S_{21}(j\Omega)|^2}\ dB, \qquad L_R(\Omega) = 10\ log[1 - |S_{21}(j\Omega)|^2]\ dB \tag{2.3}$$

Furthermore, concretely for Chebyshev filters, the transfer function follows is:

$$|S_{21}(j\Omega)|^2 = \frac{1}{1+\epsilon^2 T_n^2(\Omega)} \tag{2.4}$$

Where:

$$\epsilon = \sqrt{10^{\frac{L_{Ar}}{10}} - 1}, \tag{2.5}$$

$$T_n(\Omega) = \begin{cases} \cos(\text{n } cos^{-1}\ \Omega) & \text{if } |\Omega| \leq 1 \\ \cosh(\text{n } cosh^{-1}\ \Omega) & \text{if } |\Omega| \geq 1 \end{cases}$$

The constant ϵ is determined by the desired ripple level in the band pass.

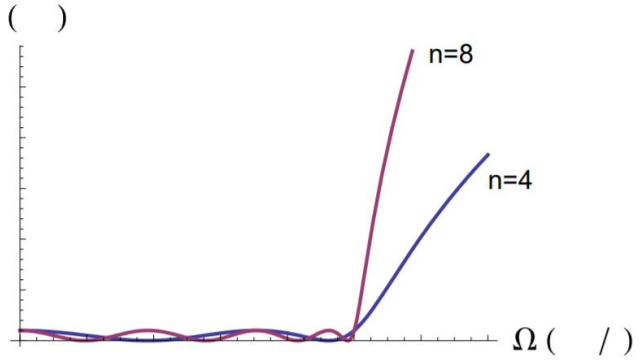

Figure 2.5: Evolution of Chebyshev Frequency Response with order n

For Elliptical filters, the transfer function can be described as:

$$|S_{21}(j\Omega)|^2 = \frac{1}{1+\epsilon^2 F_n^2(\Omega)} \tag{2.6}$$

Where:

$$\epsilon = \sqrt{10^{\frac{L_{Ar}}{10}} - 1}, \tag{2.7}$$

$$F_n(\Omega) = \begin{cases} M\dfrac{\prod_{i=1}^{n/2}(\Omega_i^2-\Omega^2)}{\prod_{i=1}^{n/2}(\Omega_s^2/\Omega_i^2-\Omega^2)} & \text{n even} \\ N\dfrac{\prod_{i=1}^{(n-1)/2}(\Omega_i^2-\Omega^2)}{\prod_{i=1}^{(n-1)/2}(\Omega_s^2/\Omega_i^2-\Omega^2)} & \text{n odd} \end{cases}$$

The frequencies Ω_i and Ω_s determine the ripple level in the pass and rejection bands.

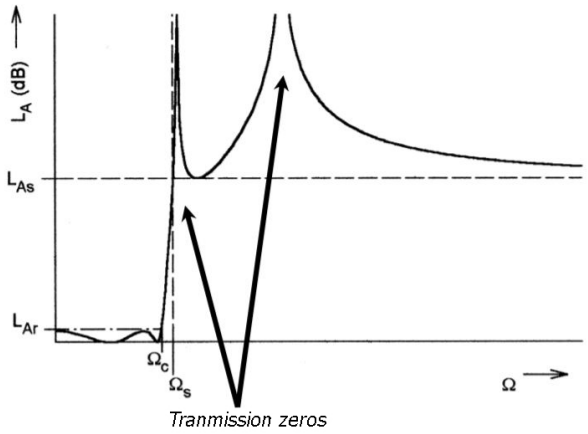

Figure 2.6: Elliptical Frequency Response

2.2.3 Lowpass Prototype

A lowpass prototype is a filter with the following characteristics:

- Its elements are normaized to obtain a source resistance of $g_0 = 1$
- The cutoff frequency of the response is $\Omega_c = 1$ rad/s
- The number of reactive elements needed is equal to the order n of the filter.

There exist two dual structure to implement lowpass prototypes. Both of them are based on L-C staircase structures.

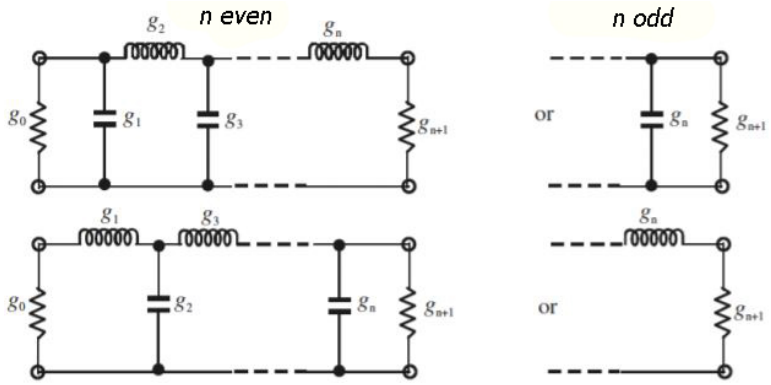

Figure 2.7: Lowpass Structures

Further procedure about this model, on how to perform a change of variable to move from lowpass to bandpass and how to undo the normalization, will be detailed in the design examples of Chaps. 4 and 5.

2.3 Microstrip Technology

Microstrip is a type of transmission line which can be manufactured using PCBs and mainly used for microwave signals transmission. It enables us to implement distributed elements that can be employed as building blocks for filter implementation.

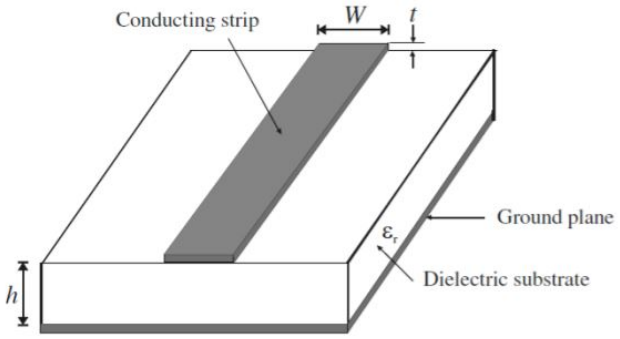

Figure 2.8: Microstrip Line

The characteristic approximated equations for synthesis and analysis are the following:

$$\epsilon_{ref} = \frac{\epsilon_r + 1}{2} + \frac{\epsilon_r - 1}{2}(1 + 12\frac{h}{W})^{-\frac{1}{2}} \tag{2.8}$$

$$Z_c = \begin{cases} \frac{60}{\sqrt{\epsilon_{ref}}} ln(2\frac{8h}{W} + \frac{W}{4h}) & \text{if } \frac{W}{h} \leq 1 \\ \frac{120\pi}{\sqrt{\epsilon_{ref}}}[\frac{W}{h} + 1.393 + 0.667ln(\frac{W}{h} + 1.444)]^{-1} & \text{if } \frac{W}{h} \geq 1 \end{cases}$$

$$\frac{W}{h} = \begin{cases} \frac{8e^A}{e^{2A}-2} & \text{assuming } \frac{W}{h} \leq 2 \\ \frac{2}{\pi}[B - 1 - ln(2B-1) + \frac{\epsilon_r - 1}{2\epsilon_r}(ln(B-1) + 0,39 - \frac{0,61}{\epsilon_r}] & \text{assuming } \frac{W}{h} \geq 2 \end{cases}$$

$$A = \frac{Z_c}{60}\sqrt{\frac{\epsilon_r + 1}{2}} + \frac{\epsilon_r - 1}{\epsilon_r + 1}(0,23 + \frac{0,11}{\epsilon_r}), \qquad B = \frac{377\pi}{2Z_c\sqrt{\epsilon_r}} \tag{2.9}$$

$$\alpha_c = \frac{R_s}{Z_c W}, \qquad \alpha_d = \frac{1}{2} w \sqrt{\mu_0 \epsilon_0}\sqrt{\epsilon_{ref}} tan\delta_{ef} \tag{2.10}$$

Chapter 3

Aggressive Space Mapping

3.1 Introduction

A widely known optimization algorithm by designers all around the world is space mapping. It is an easy and efficient way of optimizing our designs, and helps us to achieve our goal designs in a better way.

Space Mapping has different implementation varieties, but in this report, we are going to focus on Agressive Space Mapping or ASM.

"Power in simplicity", quoted from [3], the main advantage of ASM is that it is extremely efficient when the algorithm works. Basically the optimization method takes advantage of the fast and inaccurate "coarse model" which is quite easy to simulate, to find a solution for the "fine model", which is expensive to simulate, that better approximates our desired final response.

3.2 Implementation

The concept behind this technique is pretty obvious, we have two models, one which is heavy or expensive to simulate, but provides an accurate filter response, and one which is fast simulated but inaccurate, so we just want to perform a mapping between both models, so that by modifying our "fast model", we can as well compute how is our accurate model going to be altered.

This fast or **coarse model** is represented as x_c, whose frequency response is R_c. Same applies to the accurate or **fine model**, also known as x_f with a frequency response represented by R_f.

The key behind every ASM algorithm, is to generate a function **P** such that:

$$x_c = P(x_f) \tag{3.1}$$

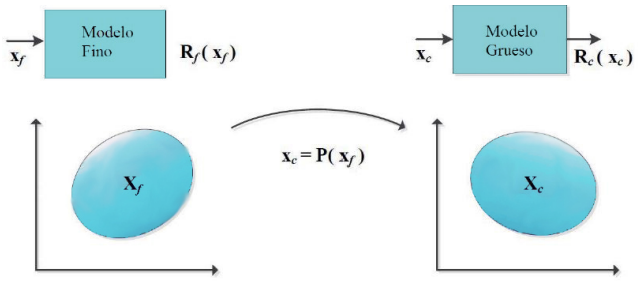

Figure 3.1: ASM Mapping Coarse and Fine Models.

The function P used to map both fine and coarse spaces in our case will be the use of parameter extraction or PE.

Having this in mind, our next concern is how to apply the method. To clarify it, all the steps have been listed in the following diagram.

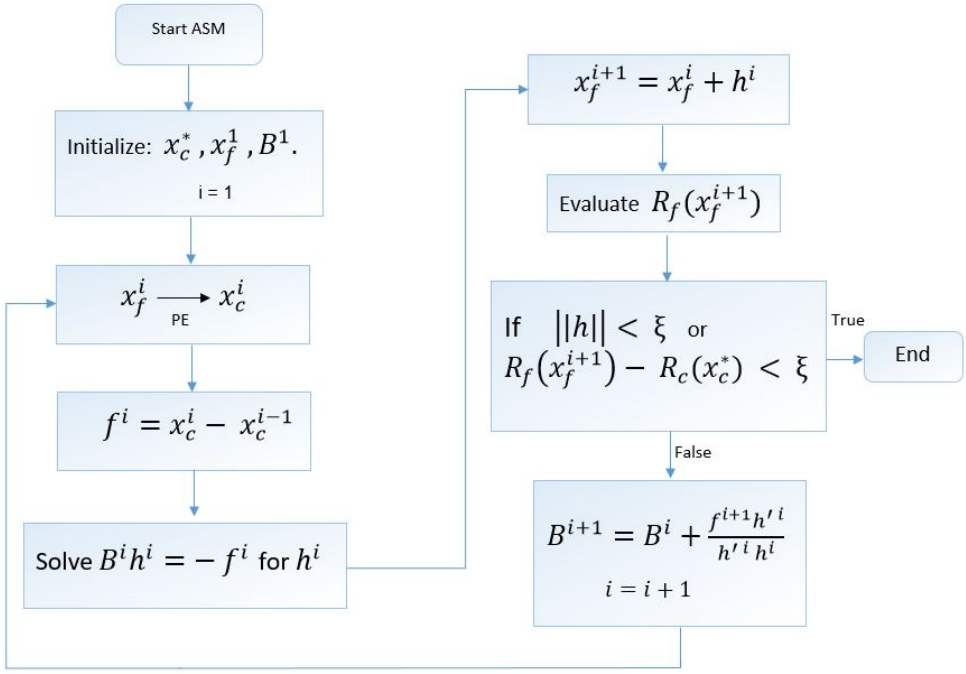

Figure 3.2: ASM Implementation Diagram.

Going on detail now, on our first step, we must compute the value of the first coarse model x_c^*, of the first fine model x_f^1 and the initial value for the Broyden matrix B, B^1.

In our case, x_c^* represents the ideal response theoretically computed for our design, x_f^1 is obtained from applying segmentation, as it will be detailed in Chaps. 4 and 5 , and in the incoming sections it will be explained how to compute Broyden matrix B as well.

Once we have computed the initial vectors and matrix, our next step is to apply parameter ex-

traction in order to obtain coarse model x_c^1 derived from our previously computed fine model x_f^1, and then, calculate the difference between this coarse model x_c^1 and our previous coarse model x_c^*.

With this difference f^1 and matrix B^1, we can solve a linear system to compute h^1, which is going to be the variation vector for our previous fine model x_f^1, so we can just compute the next fine model as : $x_f^2 = x_f^1 + h^1$.

Now, our next task is to apply an EM extraction to the new fine model x_f^2 and once we have the frequency response obtained, if we meet our chosen stop criteria, we can affirm that our algorithm is over, and if not, we have to compute our next iteration Broyden matrix B^2 and repeat the same procedure again.

3.2.1 Broyden Matrix

We have just gone over the whole implementing process of ASM algorithm, where we have seen how crucial every parameter is for the right implementation of the algorithm. Furthermore, one of its main parameters, is the Broyden matrix B, which basically models the variation that our fine model parameters will suffer, which makes it a crucial element for the algorithm correct convergence.

The main difference that ASM has, compared to other Space Mapping algorithms, is that in ASM, Broyden matrix is updated after every iteration, obtaining then a faster convergence. This fact will be true only if the updates modify the parameters towards the right direction of convergence, if not, it could end up with the algorithm failing, since it would start oscillating and never converge to our desired solution.

In Eq. 3.2, we can see the formula to compute our initial matrix B.

$$B^1 = \begin{bmatrix} \frac{\partial x_{c1}}{\partial x_{f1}} & \frac{\partial x_{c1}}{\partial x_{f2}} & \cdots & \frac{\partial x_{c1}}{\partial x_{fm}} \\ \frac{\partial x_{c2}}{\partial x_{f1}} & \frac{\partial x_{c2}}{\partial x_{f2}} & \cdots & \frac{\partial x_{c2}}{\partial x_{fm}} \\ \vdots & \vdots & \ddots & \vdots \\ \frac{\partial x_{cm}}{\partial x_{f1}} & \frac{\partial x_{cm}}{\partial x_{f2}} & \cdots & \frac{\partial x_{cm}}{\partial x_{fm}} \end{bmatrix} \tag{3.2}$$

After this initialization, the matrix B is updated with each iteration, theoretically and ideally compensating the effects that the parameters cause on each others.

As it will be seen in Chaps. 4 and 5, our starting B will be obtained from applying segmentation to our designs, and of the form:

$$B^1 = \begin{bmatrix} \frac{\partial x_{c1}}{\partial x_{f1}} & 0 & \cdots & 0 \\ 0 & \frac{\partial x_{c2}}{\partial x_{f2}} & \cdots & 0 \\ \vdots & \vdots & \ddots & \vdots \\ 0 & 0 & \cdots & \frac{\partial x_{cm}}{\partial x_{fm}} \end{bmatrix} \tag{3.3}$$

The reason for this is that at our initial point, we are going to be assuming that the variation of the parameters does not introduce changes on the others, and then, the partial derivatives are all 0 except the diagonal ones, which are the direct relation between both coarse and fine models.

3.2.2 Parameter Extraction

Described by many as the "weakest part" of the ASM technique, the PE part of the method basically consists on extracting or obtaining the coarse model parameters x_c, from the fine model frequency response $R_f(x_f)$.

The procedure to achieve this goal is to minimize the difference in frequency response of our coarse model, and our fine model, such that:

$$x_c^{(i+1)} = arg\ min\ ||R_f(x_f^{(i)}) - R_c(x_c^{(i+1)})|| \tag{3.4}$$

This is usually performed applying optimization to the coarse model. Once the difference is at its minimum, we can extract all the parameters from the coarse model schematic that the optimizer just tuned.

3.2.3 Stopping Criteria

Finally, we are going to discuss the stopping criteria of the algorithm. Here, there are mainly two approaches which are valid enough but slightly different.

The first one, consists on computing the module of the error vector h, and if it is lower than an established threshold, then the algorithm is finished.

$$||h|| < \xi \tag{3.5}$$

The main advantage of this criteria is that we make sure that the convergence of the ASM algorithm is over, because by applying the condition in Eq. 3.5, we are basically saying that the parameters variation is lower than certain threshold ($\pm$ 0.1 e.g.), which means, that our model is not going to be significantly altered any more, and we can safely stop there.

On the other hand, the second criteria comes to the point of computing the error between the frequency response of our fine model $R_f(x_f)$ and our desired ideal frequency response. If the error is less than a set threshold, then our approximation is good enough and we do not need to perform any further iterations. This criteria is also very solid, and it is recommended to be adopted on designs where the convergence of the model is not really clear to happen (compact designs where the variations of some parameters heavily affect others, designs with a high filter order, transmission zeros..).

$$R_{ideal} - R_f(x_f) < \xi \tag{3.6}$$

In our case, as we will see in further chapters, we are going to be using both criteria, each one for one of the designs, depending on which one fits better in every occasion.

3.3 Analysis of ASM Convergence.

In this last section, a thorough analysis will take place, showing how much does the algorithm differ when computing the initial point in different ways.

As it has been explained before, the main objective of ASM is to map both the coarse and fine models, so that by applying changes over the coarse model, we can easily obtain the equivalent change on the fine model. All this process is done because the fine model takes long and is hard to simulate, whereas the coarse model, is more inaccurate but easy and fast to simulate.

Having this in mind, It was previously stated that the initial point for our fine model, as well as the characteristic curves needed to initialize the Broyden matrix B, were obtained following a segmentation technique. But this raises the following question, which approach should we use when applying this technique to our design?

Because we can either opt for the fast simulations or for the heavy EM simulations and the results, slighter or major, will differ.

It should be noted that for this study, the design of Chap. 4 has been used, to simulate the coarse and fine models, AWR's circuital simulator and EM extractions have been applied respectively.

In first place, we are going to analyze the variation of the initial point parameters in both models, and then a comparison of the characteristic curves for each of them will be discussed.

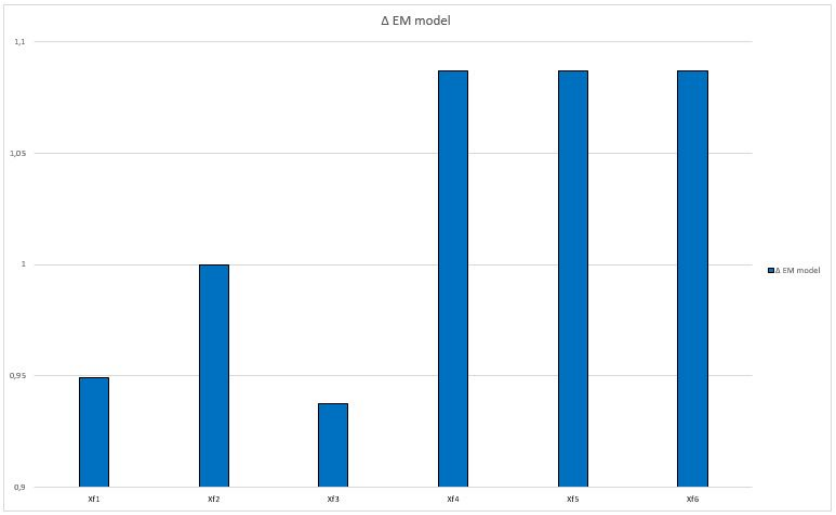

Figure 3.3: Normalized Variation of EM Simulated Initial Parameters.

In Fig. 3.3, we can appreciate the normalized variation of the EM-simulated parameters with respect to the circuital ones, which as it can be observed, is always in between $\pm$ 10 %, what does not mean a really huge change, but still can mean a difference to the algorithm.

Now, we will proceed to compare the characteristic curve for each parameters.

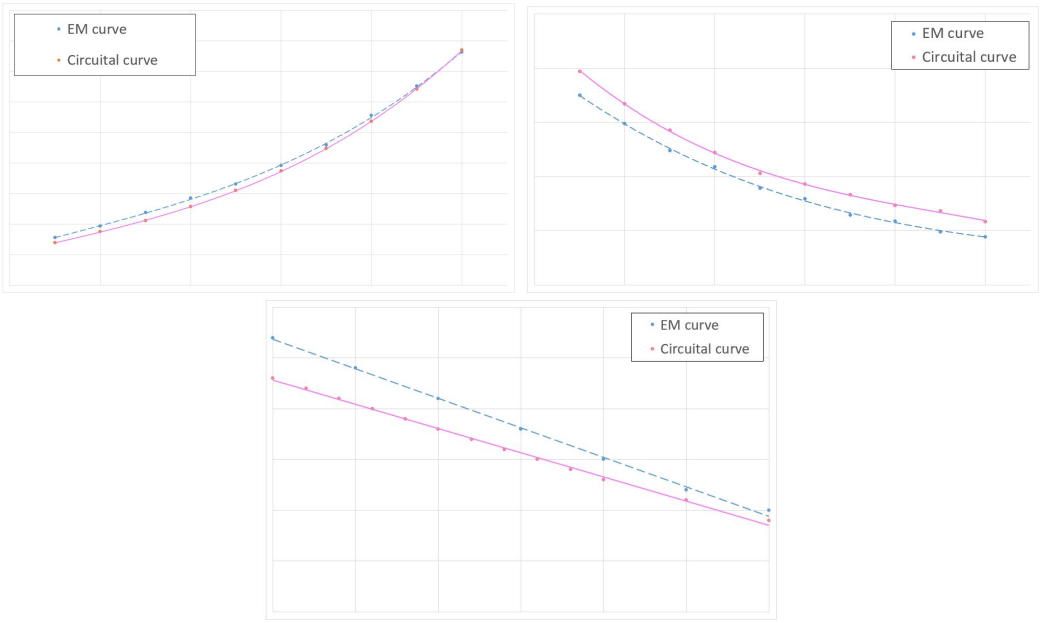

Figure 3.4: EM Simulated Curves vs Circuital Simulated Curves.

It can be clearly seen how the circuital curve approximates the EM one really well, and what is more, with a similar slope, what means that the partial derivatives needed to initialize B matrix will have almost similar values as well.

Difference on matrix B can be noted in Eq. 3.7.

$$\Delta B = \begin{bmatrix} +5.2\% & 0 & 0 & 0 & 0 & 0 \\ 0 & 0\% & 0 & 0 & 0 & 0 \\ 0 & 0 & -6.25\% & 0 & 0 & 0 \\ 0 & 0 & 0 & +8.7\% & 0 & 0 \\ 0 & 0 & 0 & 0 & +8.7\% & 0 \\ 0 & 0 & 0 & 0 & 0 & +8.7\% \end{bmatrix} \tag{3.7}$$

Where, again, our EM deviation compared to the circuital one, is less than 10%.

With all these facts, we could predict that initializing the ASM algorithm using circuital or EM simulations to obtain the parameters, would not have an enormous impact on the final convergence of the method, maybe it would delay it, but at the end, we would probably end up on the same point using one approach or the other.

But to be sure of this, we are going to apply some iterations of the ASM algorithm and see, how far are both models from each other.

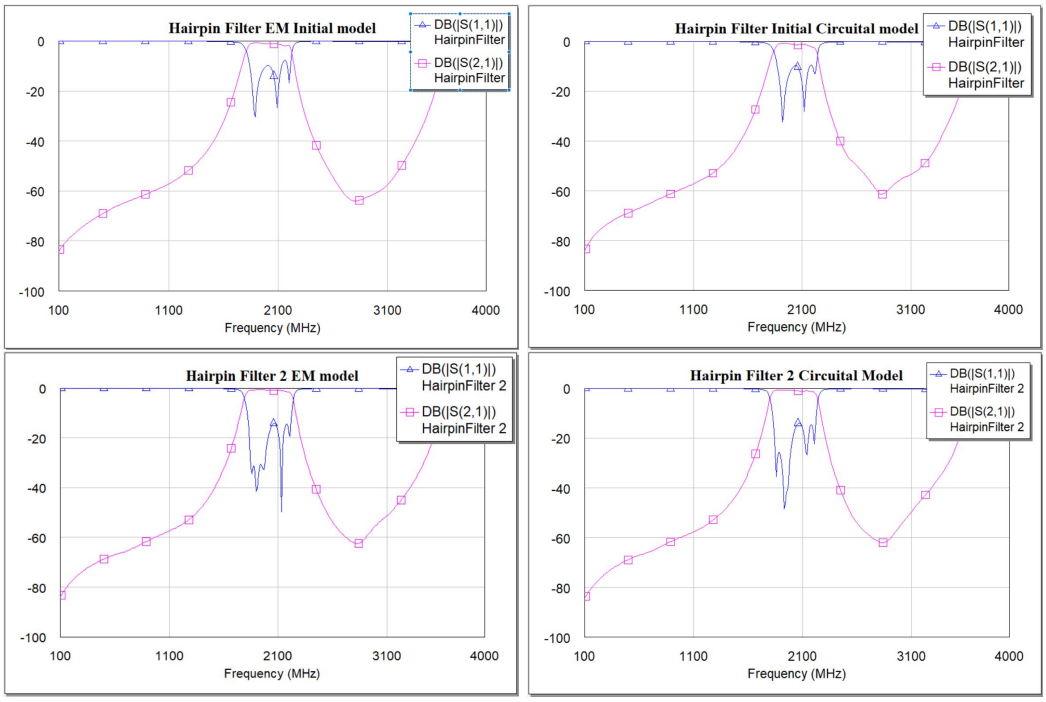

Figure 3.5: EM Simulated vs Circuital Simulated Convergence.

As it can be clearly appreciated in Figs. 3.5, the initial point is really close, and after three iterations, the convergence of the design is also quite close. It should be noted that in "Hairpin Filter 2 EM model" graph, the return losses S_{11}, present a coupling between two resonators, which causes the negative pike, but despite this fact, both models convergence is quite similar.

So after all these analysis, we can conclude that both circuital or EM approaches are valid to initialize ASM algorithm, and may only affect to how fast wil the method convergence, but still will not make a huge difference.

Having said this, for our design example, we are going to follow circuital approaches, which makes our design time much lower, since the circuit simulations are almost instantaneous and we can obtain all the desired parameters in a really short period of time.

Chapter 4

Design Example 1: Hairpin Filter

4.1 Introduction

Once all the theoretical concepts needed for the development of this project were covered, the next step was to implement our real designs, and test how the ASM optimization algorithm would behave in a real model. For this very first design, a hairpin resonator based filter example found in [1] was followed.

4.2 Theoretical design

In this part we can distinguish between two different theoretical subsections, the coarse model or circuital one and the fine model or microstrip one. Lets start with the microstrip one.

4.2.1 Microstrip theoretical calculations

Our first goal will be to theoretically compute the dimensions which are going to be required for the microstrip lines of our fine models and of course, final design. In order to compute these values, we need the parameters of the substrate. In this case, Rogers 4003C was chosen for our designs, which has an ϵ_r value of 3.55 and a thickness T of 1.51 mm. With the following characteristic equations for microstrips we can compute the parameters that we need in order to continue with our design.

We will fix a width W for our microstrip lines of 2.04 mm as well.

$$\epsilon_{ref} = \frac{\epsilon_r + 1}{2} + \frac{\epsilon_r - 1}{2}(1 + 12\frac{h}{W})^{\frac{-1}{2}}, \qquad \lambda_g = \frac{c_0}{f\sqrt{\epsilon_{ref}}}, \qquad L_{tot} = \frac{\lambda_g}{2}, \tag{4.1}$$

A hairpin resonator is just a $\frac{\lambda}{2}$ straight resonator folded by its half, so by applying Eq. 4.1, we

obtain a total resonator length L_{tot} of 46.5 mm.

In addition, and using AWR's T_x Tool, we compute the impedance of our microstrip lines, which in this case is $Z_c = 66.7\ \Omega$.

Furthermore, our filters will be designed to have an input/output impedance Z_0 of 50 ohms, so with the help of the same tool, the input/output microstrip lines width W_0 is 3.31 mm.

4.2.2 Circuital theoretical design

As mentioned before, the example found at [1] establishes the following specifications for this bandpass Chebyshev filter:

Specifications			
n	f_0	FBW	Ripple
5	2 GHz	0.2	0.1 dB

Table 4.1: Hairpin Filter Design Specifications.

With these requirements, our next step is to calculate the ideal frequency response of the filter. In order to do this, it will be first designed the lowpass model of itself. Once we have correctly designed the lowpass prototype, we will perform a change of variable over the capacitors and inductors values, in order to shift the filter response to the central frequency f_0.

n	g_1	g_2	g_3	g_4	g_5	g_6
1	0.3052	1				
2	0.8431	0.622	1.3554			
3	1.0316	1.1474	1.0316	1		
4	1.1088	1.3062	1.7704	0.8181	1.3554	
5	1.1468	1.3712	1.975	1.3712	1.1468	1

Table 4.2: Chebyshev Lowpass Model Coefficients for $L_{ar} = 0.1$ dB.

From Tab. 4.2 we can obtain our lowpass prototype coefficients for n=5. The next step is to apply the correspondent change of variable to the inductors and capacitors.

$$\Omega = \frac{\Omega_c}{\Delta w}\left(\frac{w}{w_0} - \frac{w_0}{w}\right) \tag{4.2}$$

By applying Eq. 4.2, we obtain the following results:

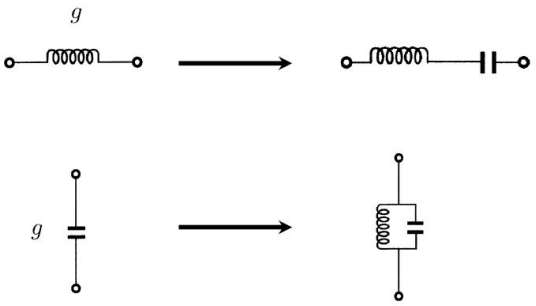

Figure 4.1: Transformation from lowpass to bandpass prototype.

Where the correspondent values of L_s, C_s, L_p and C_p can be computed with these equations:

$$L_s = (\frac{\Omega_c}{\Delta w \cdot w_0})Z_0 g, \qquad C_s = (\frac{\Delta w}{\Omega_c w_0})\frac{1}{Z_0 g}, \qquad L_p = (\frac{\Delta w}{\Omega_c w_0})\frac{Z_0}{g}, \qquad C_p = (\frac{\Omega_c}{\Delta w \cdot w_0})\frac{g}{Z_0} \tag{4.3}$$

Being $\Delta w = \frac{w_2 - w_1}{w_0}$ and $w_0 = \sqrt{w_1 w_2}$ in equations 4.3. Finally, our impedance Z_0 is going to be set at 50 Ω, which will also be the impedance of the input and output ports. With all this information, we are now able to compute our component values.

Z0(Ω)	L_{1_s}(nH)	C_{1_s}(pF)	L_{2_p}(nH)	C_{2_p}(pF)	L_{3_s}(nH)	C_{3_s}(pF)
50	22.81	0.2776	0.5803	10.91	39.29	0.1612

Table 4.3: Capacitors and Inductors values for Bandpass Model.

There is no need to compute the value of the last two LC resonators, since the filter is symmetric and the values are exactly the same as the ones for the first and second resonators. The following model is obtained:

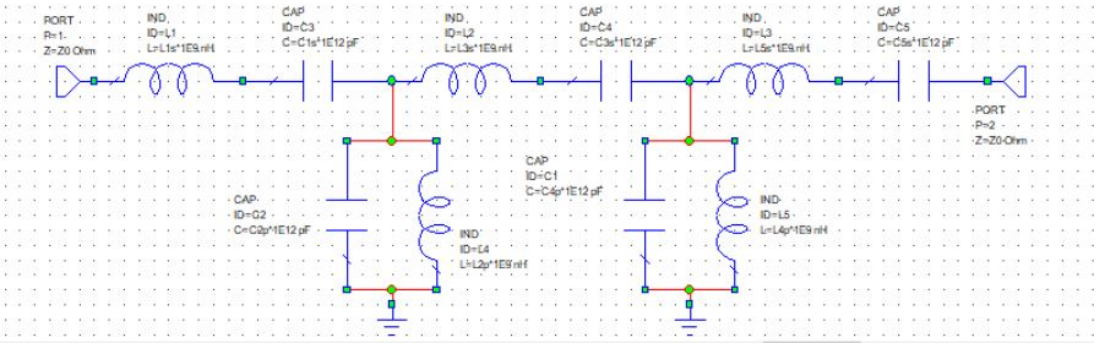

Figure 4.2: Chebyshev Bandpass Ideal Model.

But even though the model in Fig. 4.2 is already an ideal model, it is not our final ideal model. The next step, is to replace the resonators by its equivalent J admittance inverter in series plus an RLC

parallel resonator. The reason why we need to do this, is because we need to convert all the resonators from series to parallel, to be able to physically manufacture them, and we add the R component to the resonators to add the effect of the losses. Furthermore, instead of using the previously computed values for L and C, we are going to fix the value of C for all the resonators with the help of equation 4.4, which can be found in [1] and which gives us the capacitance value for our filter. Note that for our initial ideal model, all five resonators are going to be equal.

$$C_{res} = \frac{\pi}{2 \cdot 2\pi f Z_c} \tag{4.4}$$

It must be remarked that Z_c is the value for the characteristic impedance of the microstrip model, computed in previous subsection. Variations on the resonator frequency, will be translated into inductance L changes, which will be computed using equation 4.5

$$L_{res_i} = \frac{1}{(2\pi f_i)^2 C_{res}} \tag{4.5}$$

As previously stated, to model the filter losses, we will add a resistance value R_{res} which can be calculated as:

$$R_{res} = w_0 * L_{res} * Q_0 \tag{4.6}$$

Where Q_0 is the quality factor of the filter.

This whole previous step is crucial, because by fixing the capacitance C, we fix the slope parameter of the filter, so now we can freely allow the ASM algorithm tune the frequency of the resonators, the external quality factor and the coupling coefficients in order to optimize our design, because once we have computed the initial point for the algorithm, it will be valid for every single iteration. If we did not fix the slope parameter, for every iteration, we would be modifying the ASM starting point, since for a new C value, we would have different parameter curves, and ASM algorithm would never converge. Despite this fact, the value for the inductors L will be different in each resonator, since it depends on the frequency of the resonator among other variables and constants, and this parameter will be modified through each of the ASM iterations.

Having said this, we can now compute the values of our J admittance inverters by using equations 4.7

$$J_{01} = \sqrt{\frac{FBW w_0 C_{res}}{Z_0 g_0 g_1}}, \qquad J_{i,i+1} = \frac{FBW w_0 C_{res}}{\sqrt{g_i g_{i+1}}} \tag{4.7}$$

By applying these equations, we obtain the following ideal values:

Ideal Model Params					
J_{01}	J_{12}	J_{23}	$R_{res}(\Omega)$	$C_{res}(pF)$	$L_{res}(nH)$
0.009104	0.00379	0.002888	7154	1.89	3.349

Table 4.4: Theoretical values.

The final ideal schematic is presented in Fig 4.3.

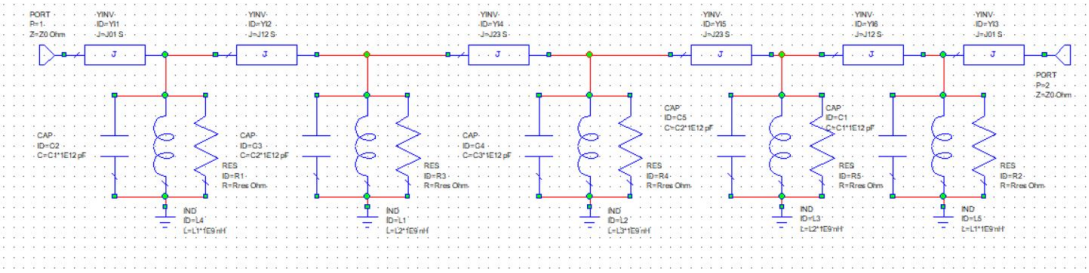

Figure 4.3: Chebyshev Bandpass Final Ideal Model.

And finally, the ideal frequency response can be observed in Fig 4.4.

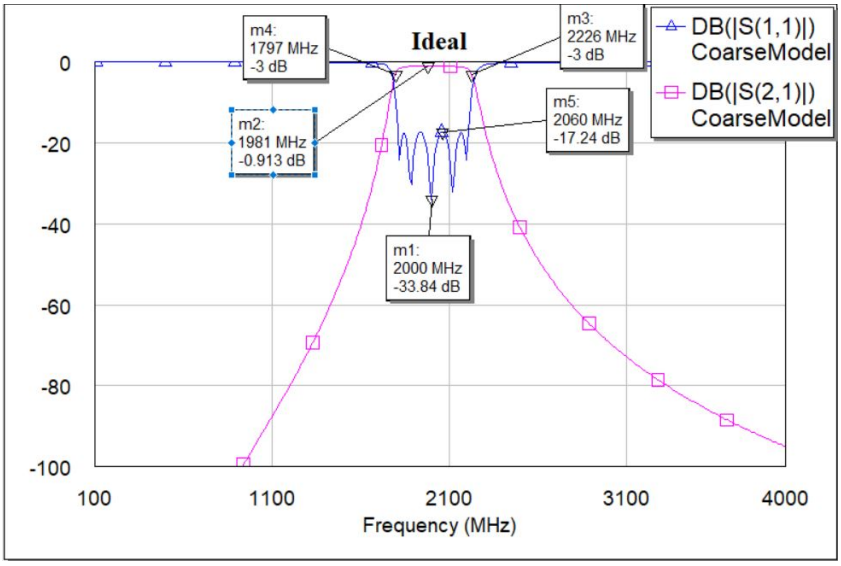

Figure 4.4: Chebyshev Bandpass Ideal Frequency Response.

Where it can be appreciated how the filter is correctly centered at 2 GHz, and has an appropriate return and transmission losses level of $S_{11} = -17.24$ and $S_{21} = -0.913$ dBs correspondingly, due to the effect of losses introduced by R_{res}.

Finally, we will compute the theoretical values of Q_{ext} and coupling coefficients k_{12} and k_{23}.

$$Q_{ext} = \frac{w_0 C_{res}}{Z_0 J_{01}^2}, \qquad k_{i,i+1} = \frac{J_{i,i+1}}{w_0 C_{res}} \tag{4.8}$$

With help of Eq. 4.8 we obtain a value of 5.734 for Q_{ext}, 0.1595 for k_{12} and 0.1215 for k_{23}.

We can now move on to our next task, which is going to be, applying segmentation to our fine model, or in other words, our bandpass filter implemented using microstrip lines.

4.3 Segmentation process

Before moving to our microstrip or fine model, we need to choose which are going to be the parameters of the filter which will be used for the ASM optimization technique. For this example, we will allow ASM to tune the value of the external quality factor Q_{ext}, the three different resonator frequencies, $f_1 = f_5$, $f_2 = f_4$ and f_3, and the two gaps, $g_1 = g_4$ and $g_2 = g3$, which sum up to six parameters in total, and also are the main frequency response modifiers. Translated to the fine model, these parameters represent the tapping t or entry point into the filter, the three lengths of the hairpin resonators L_h, and the physical separation between them $s_1 = s_4$ and $s_2 = s_3$. So, with everything set up, we can proceed, apply segmentation and start analyzing our fine model part by part.

First things first, before starting segmentation, we need to build our hairpin resonator. To achieve this task, we are going to help ourselves on the previously calculated filter values. In addition, to modify the resonator frequency, we are going to vary the central length of itself, notoriously simplifying the design process for us, since the rest of the parameters will not be considerably affected.

By convention, we are going to start with a central length L_h of 4.6 mm. This value is chosen because it is not recommended to have a central length much lower than twice the width of the microstrip line W, of 2.04 mm in this case, but we also need some margin to change this length while applying ASM techniques. In addition, we will choose a radius R_c of 2 mm as well, enough to have a decent curvature in the layout. Finally, the input line will have a length of 5 mm.

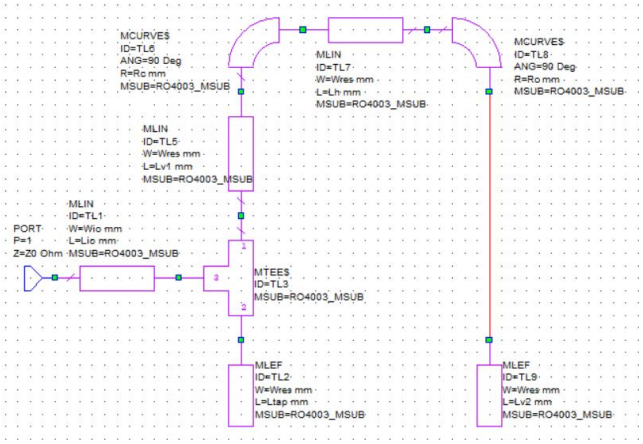

Figure 4.5: Hairpin Resonator Schematic.

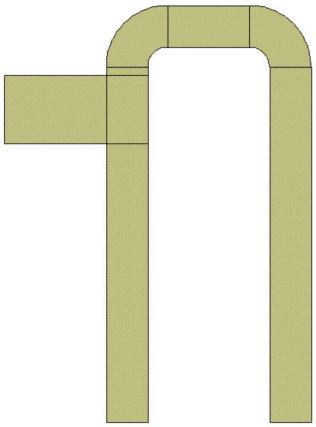

Figure 4.6: Hairpin Resonator Layout.

The schematic has been designed using AWR's components MLIN, MLEF, MTEE$ and MCURVES as it can be observed in Fig. 4.5. The total length of the resonator can be calculated as:

$$L_{tot} = 2 \cdot L_{side} + \pi \cdot R_c + L_{h0} \tag{4.9}$$

And for the input side, the length can be computed as:

$$L_{input-side} = L_{side} - W_{in} - L_{tap} \tag{4.10}$$

By doing this, we can now vary our tapping point and the hairpin resonator total length will not be modified.

The last thing to do before starting the parameter extraction, is to center our resonator at 2 GHz, in order to do this we will vary to total length of the resonator to move the resonating frequency to our desired frequency. This process will be carried out by looking at its group delay graph, appreciated in Fig. 4.7. After doing this, we obtain a L_{tot} value of 45.12 mm.

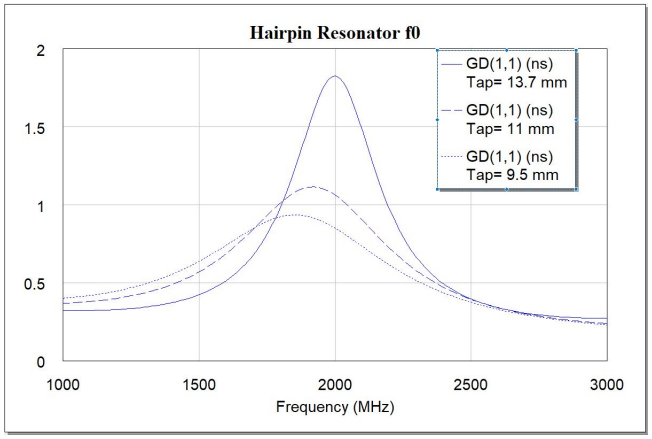

Figure 4.7: Hairpin Resonator's Group Delay Graph.

After applying these changes, we can start analyzing each parameter. To obtain Q_{ext} characteristic curve, we just need to vary the value of the tapping parameter as defined in 4.10, and measure how does the group delay of the resonator changes with the tapping variations.

$$Q_{ext} = \frac{2 \cdot \pi g df_0}{4} \tag{4.11}$$

With the measurements from the group delay graph, and equation 4.11, the following characteristic curve is obtained.

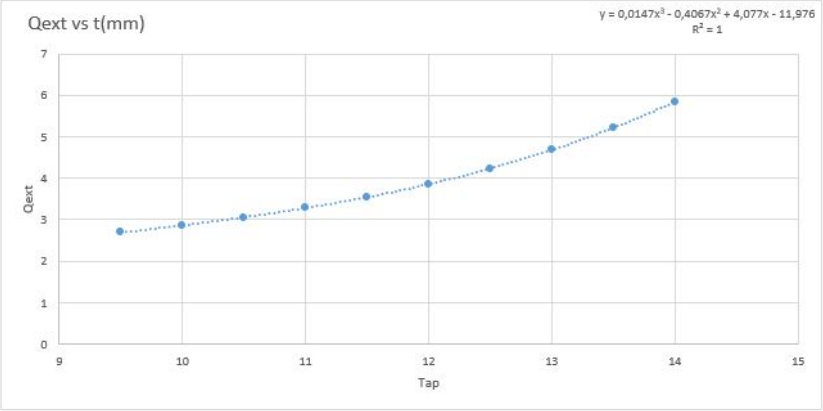

Figure 4.8: Tapping vs Q_{ext} characteristic curve.

From this graph, and in order to achieve our theoretically calculated goal Q_{ext} of 5.7, we need to fix a tapping value t of 13.7 mm.

Now we can move on to the next parameter to be analyzed. Using the same schematic as before, we can obtain the curve relating the variation in frequency f associated to the central length of the resonator L_h.

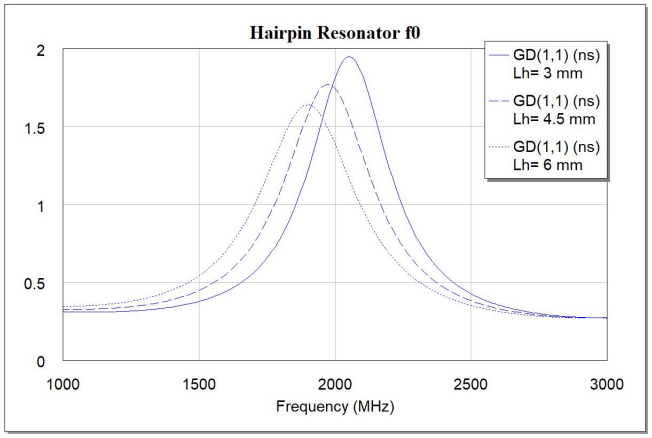

Figure 4.9: Hairpin Resonator's Group Delay Graph depending in Length.

To obtain this curve, we just need to focus on the f_0 value of Fig. 4.9. The following curve characterizes this relation:

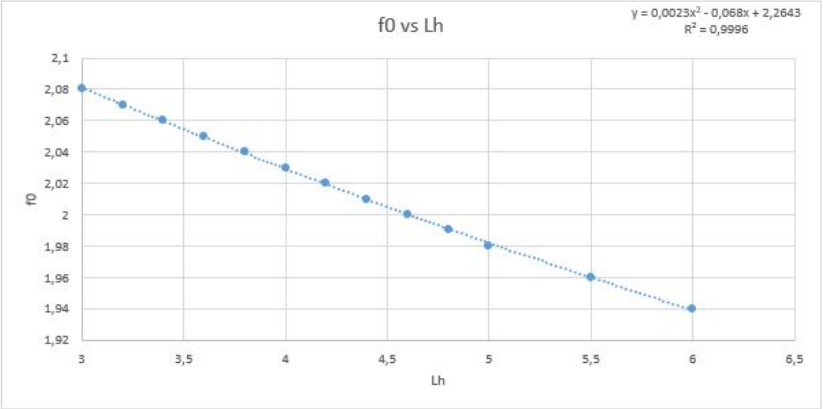

Figure 4.10: f_0 vs L_h characteristic curve.

In order to achieve the initial objective of $f_0 = 2$ GHz, we must fix all three L_h initial values at 4.6 mm.

With this step completed, we are now more than halfway through our initial point calculation. The next task will be to obtain the curve for the k_{ij} parameter in terms of the physical gap s.

To be able to compute this curve, we are going to build an schematic with two hairpin resonators flipped with respect to each other and coupled. For the coupling, the M2CLIN component has been used, which directly allows us to set the desired gap and coupling line length. The last step before starting simulating is to decouple both entry and exit ports, what was easily solved adding a gap of 0.2 mm in each of the filter ports.

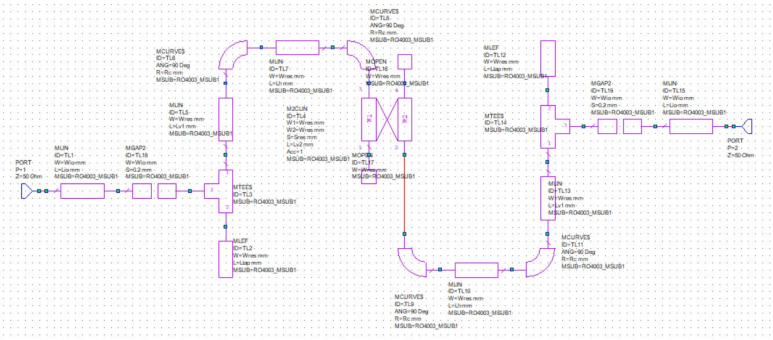

Figure 4.11: Schematic for measuring gap s vs k_{ij} curve.

The schematic has been designed reusing the previous schematic from Fig. 4.5 and adding the AWR components MOPEN and M2CLIN.

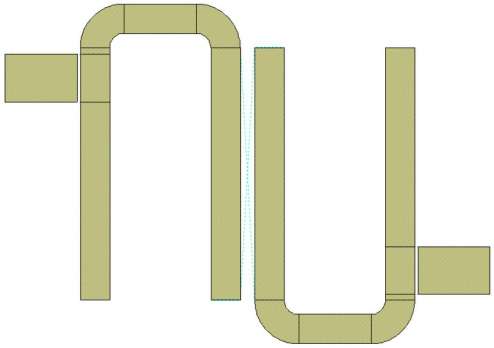

Figure 4.12: Schematic Layout.

Now we can just plot the scattering parameter S_{21} of the new schematic. The following graph was obtained:

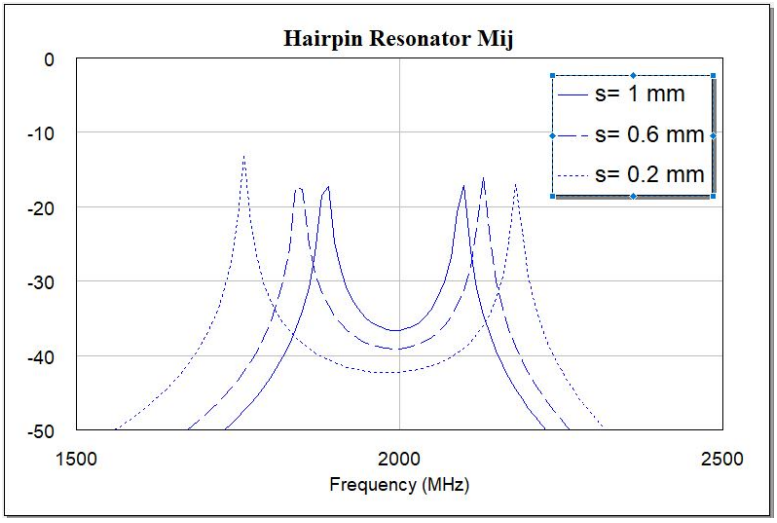

Figure 4.13: S_{21} vs s graph.

And from this graph, by applying Eq. 4.12, we can obtain the k_{ij} values, and furthermore, the characteristic curve.

$$k_{ij} = \frac{f_2^2 - f_1^2}{f_2^2 + f_1^2} \tag{4.12}$$

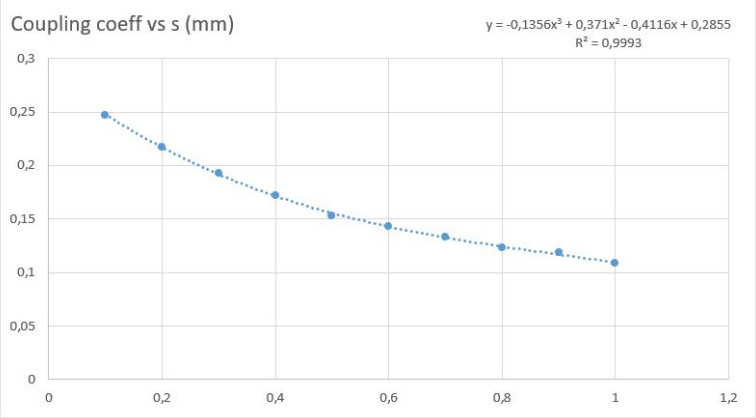

Figure 4.14: Gap s vs k_{ij} characteristic curve.

For our k_{ij} values of 0.16 and 0.122, the gaps s_1 and s_2 have values of 0.45 and 0.8 mm respectively.

With this final curve obtained, we have finished our initial point calculation.

Finally, we can now set up our whole filter schematic, and perform an EM extraction to check if the EM frequency response is good enough to be used as a starting point for the ASM algorithm.

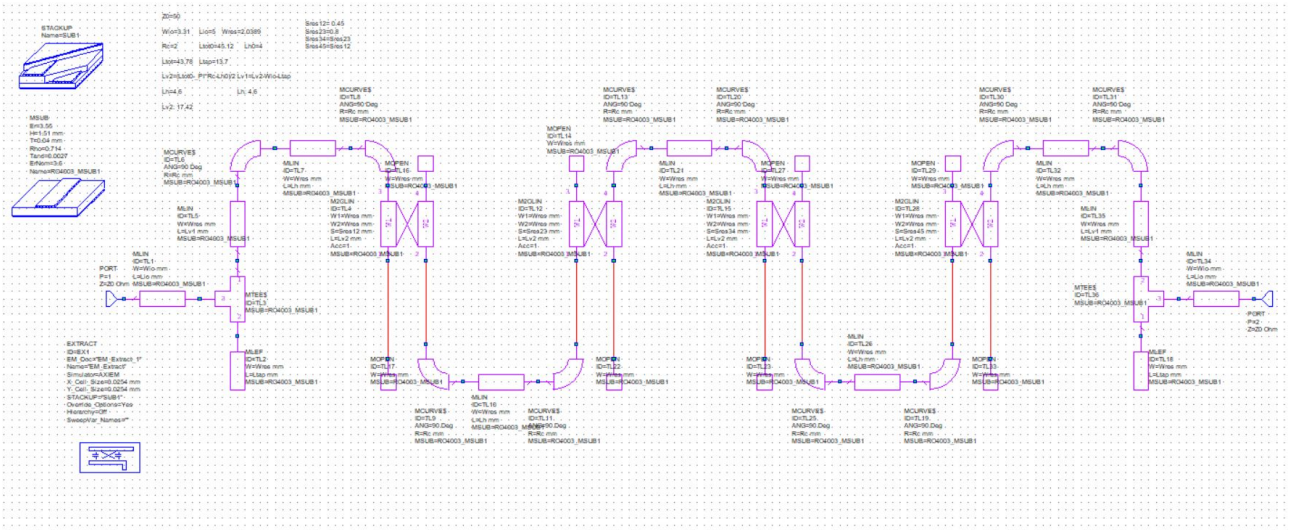

Figure 4.15: Fine Model First Approach Schematic.

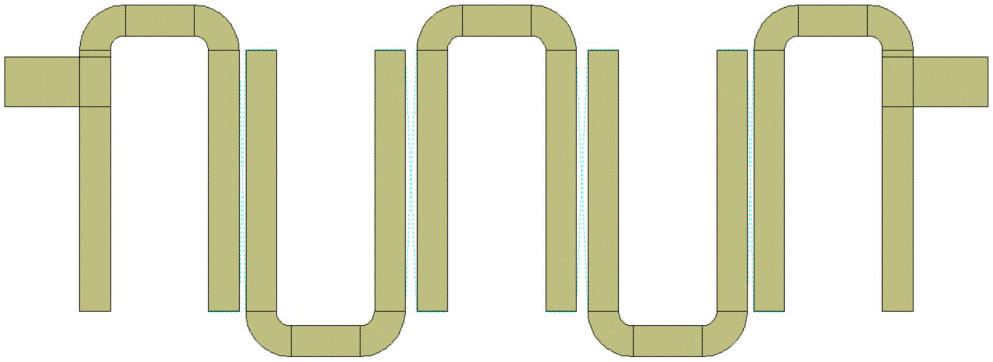

Figure 4.16: Fine Model First Approach Schematic Layout.

To be able to perform the EM extraction and simulation, we need to enable that option in each component properties. In addition, we need to have an stackup defined for our substrate to perform this action. After doing this, we can now set up a new graph for our fine model, with the scattering parameters S_{21} and S_{11} and check the obtained results.

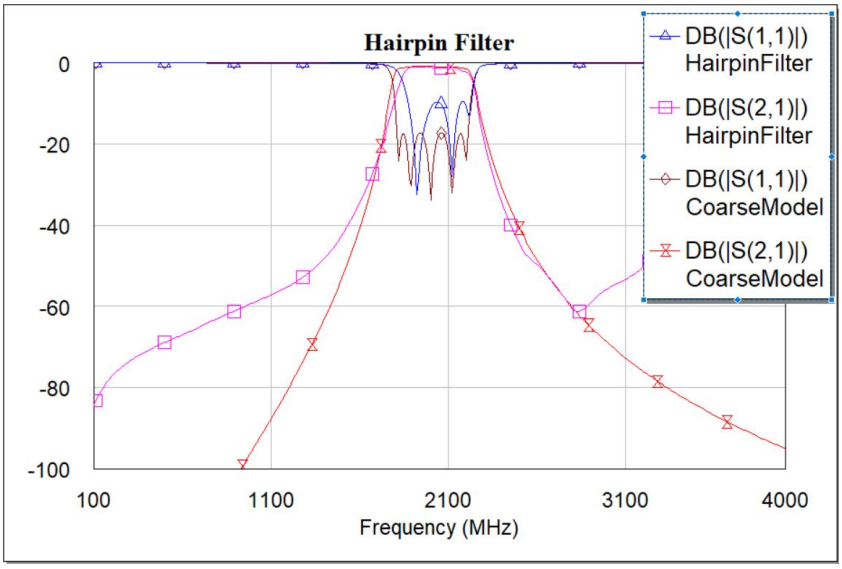

Figure 4.17: Fine Model Initial Point EM Simulation.

The initial point is good enough as it can be observed in Fig. 4.17. So we can now proceed to configure our ASM algorithm and start applying it.

4.4 ASM Optimization

Since we have already computed our initial fine and coarse models $x_c = [Q_{ext}, k_{12}, k_{23}, f_1, f_2, f_3]$ and $x_f = [tap, s_1, s_2, L_{h1}, L_{h2}, L_{h3}]$, our very last task to finish before starting applying the ASM

algorithm is to compute the values for the Broyden matrix B described in Chap. 3.

These values are the tangent lines to the previously plotted characteristics curves at the initial point, so we need to obtain the partial derivative values of each curve.

So, from Figs 4.8, 4.10 and 4.14, we obtain the approximated polynomials to the curves. These polynomials and its own partial derivatives are presented in the following equations:

$$Q_{(t)} = 0.0147t^3 - 0.4067t^2 + 4.077t - 11.976, \qquad \left.\frac{\partial Q}{\partial t}\right|_{t=13.7mm} = 1.21 \tag{4.13}$$

$$kij_{(s)} = -0.1356s^3 + 0.371s^2 - 0.4116s + 0.2855, \qquad \left.\frac{\partial kij}{\partial s}\right|_{s_{1,2}=0.45,\ 0.8mm} = -0.16, -0.078352 \tag{4.14}$$

$$f_{(l)} = -0.0589l^3 + 0.2241l^2 - 0.3263l + 0.2553, \qquad \left.\frac{\partial f}{\partial l}\right|_{l=4.6mm} = -0.04684 \tag{4.15}$$

Once we have completed these calculations, it is time to build our B matrix, which is going to be a 6x6 matrix.

$$B = \begin{bmatrix} 1.21 & 0 & 0 & 0 & 0 & 0 \\ 0 & -0.16 & 0 & 0 & 0 & 0 \\ 0 & 0 & -0.078352 & 0 & 0 & 0 \\ 0 & 0 & 0 & -0.04684 & 0 & 0 \\ 0 & 0 & 0 & 0 & -0.04684 & 0 \\ 0 & 0 & 0 & 0 & 0 & -0.04684 \end{bmatrix} \tag{4.16}$$

As it was previously stated, a Python script to simplify parameter calculations trough ASM iterations, and to keep track of all these values, was developed. In order to compute the next fine model, we need to compute a few things, the Broyden matrix B, which we already did, the previous coarse model x_c^*, or our first ideal model in this case, the previous fine model x_f^1, which we built applying segmentation, and the coarse model x_c^1 obtained applying PE to match the initial fine model, which we have not obtained yet.

So to compute this model, we duplicate our ideal coarse model schematic, and create an error graph comparing it against our initial fine model.

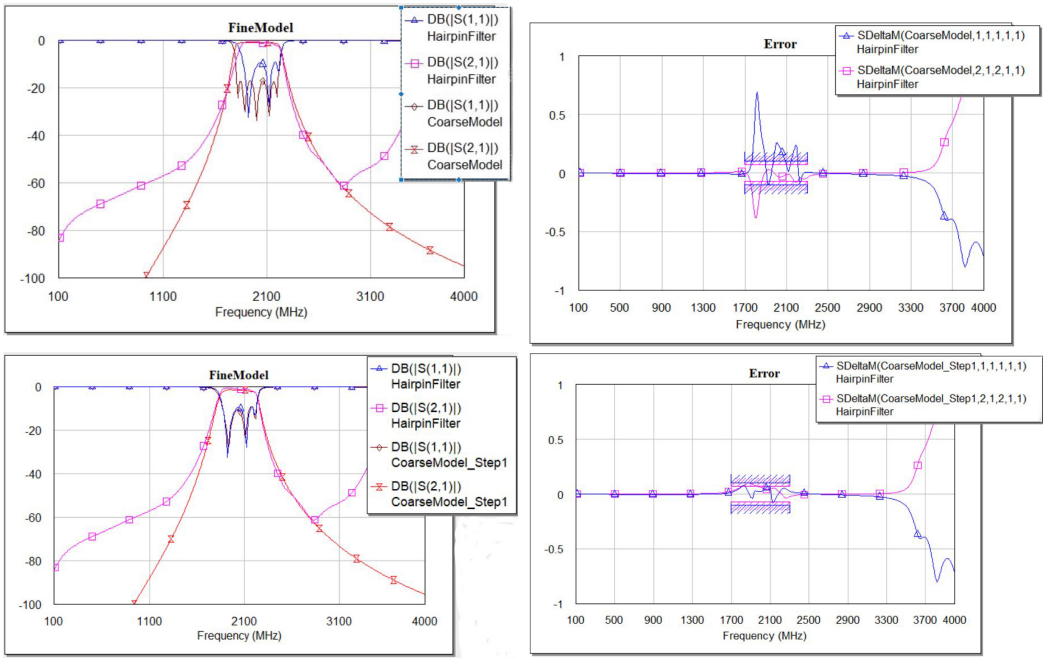

Figure 4.18: Fine Model vs Coarse Model Step 1 PE Process.

The optimization goals used were the following:

	$S\Delta M_{1,1}$	$S\Delta M_{2,1}$
$>$	0.1	0.07
$<$	0.1	0.07

Table 4.5: Optimization Goals.

And by using some powerful optimizer such as Simplex(local) or diff. eq. evolution, we reduce the error between frequency response of coarse model x_c^1 and the frequency response of fine model x_f^1, as it can be seen in 4.18.

Now, we extract Q_{ext}, k_{12}, k_{23}, f_1,f_2 and f_3 parameters from the new coarse model x_c^1 schematic and with these values, we have everything we need in order to apply ASM. All the required parameters are introduced into the script and the following output is obtained:

```
This is iteration: 1
Previous coarse model:
[5.734 ,0.1595,0.1215,2.    ,2.    ,2.    ]
Fine model:
[13.7 , 0.45, 0.8 , 4.6 , 4.6 , 4.6 ]
New coarse model to match fine model:
```

```
[4.97  ,0.1565,0.1127,1.9541,2.0283,2.03  ]
Previous h vector:
[0,0,0,0,0,0]
New h vector:
[ 0.631405 ,-0.01875  ,-0.1123137,-0.9799317, 0.6041845, 0.6404782]
Matrix B:
[[ 1.21    , 0.      , 0.      , 0.      , 0.      , 0.      ],
 [ 0.      ,-0.16    , 0.      , 0.      , 0.      , 0.      ],
 [ 0.      , 0.      ,-0.078352, 0.      , 0.      , 0.      ],
 [ 0.      , 0.      , 0.      ,-0.04684 , 0.      , 0.      ],
 [ 0.      , 0.      , 0.      , 0.      ,-0.04684 , 0.      ],
 [ 0.      , 0.      , 0.      , 0.      , 0.      ,-0.04684 ]]
New fine model:
[14.331405 , 0.43125  , 0.6876863, 3.6200683, 5.2041845, 5.2404782]
Error:
1.4653175283711695
```

In the previous output, the value of xc_0, xc_1, xf_0, xf_1, B and the error can be remarked, since they are the references for the ASM evolution.

Once we have this, we can build the next fine model x_f^2, with the new dimensions obtained by our scripts, perform another EM extraction, and plot the resulting scattering parameters or frequency response. Now we just need to repeat the same procedure again and again and let ASM algorithm converge to a desired frequency response.

In the following figures we are going to witness and analyze the evolution of all the different parameters, dimensions, and frequency responses through iterations.

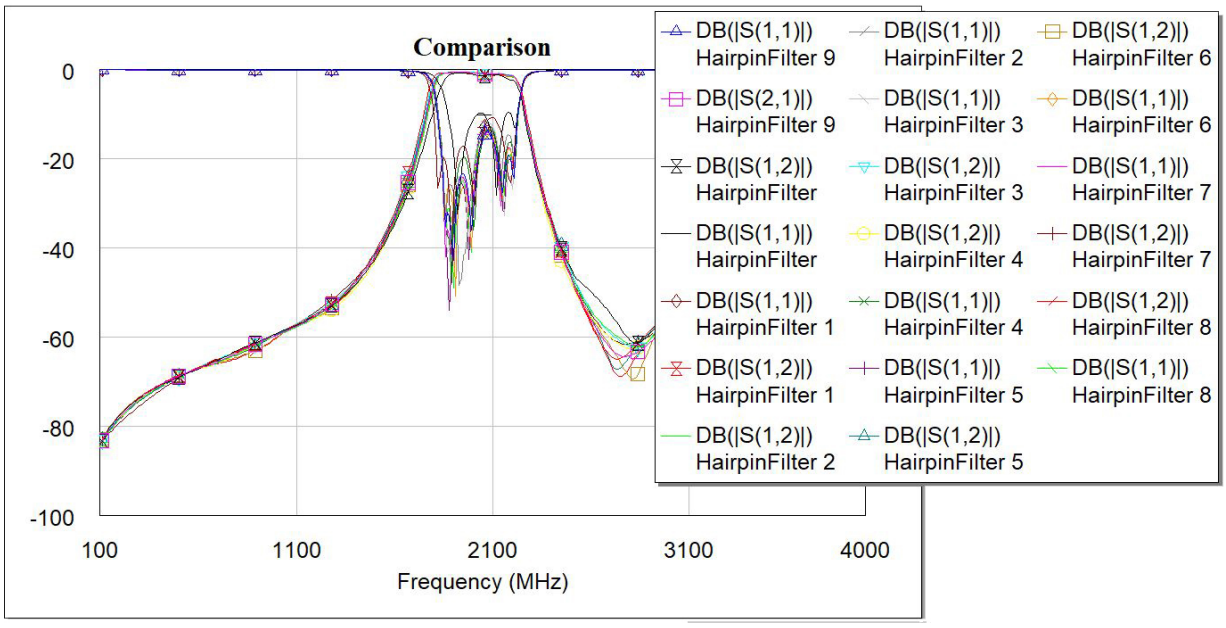

Figure 4.19: Evolution of Frequency Response with each Iteration.

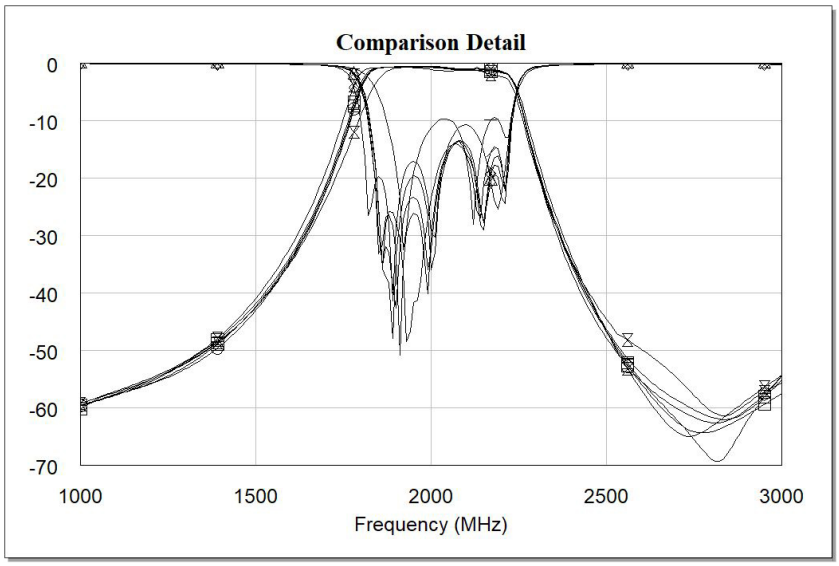

Figure 4.20: Gradient of Freq Response.

In Figs. 4.19 and 4.20, it can be appreciated how the model converges to certain frequency response.

Lets observe now the evolution of the parameters and ASM error.

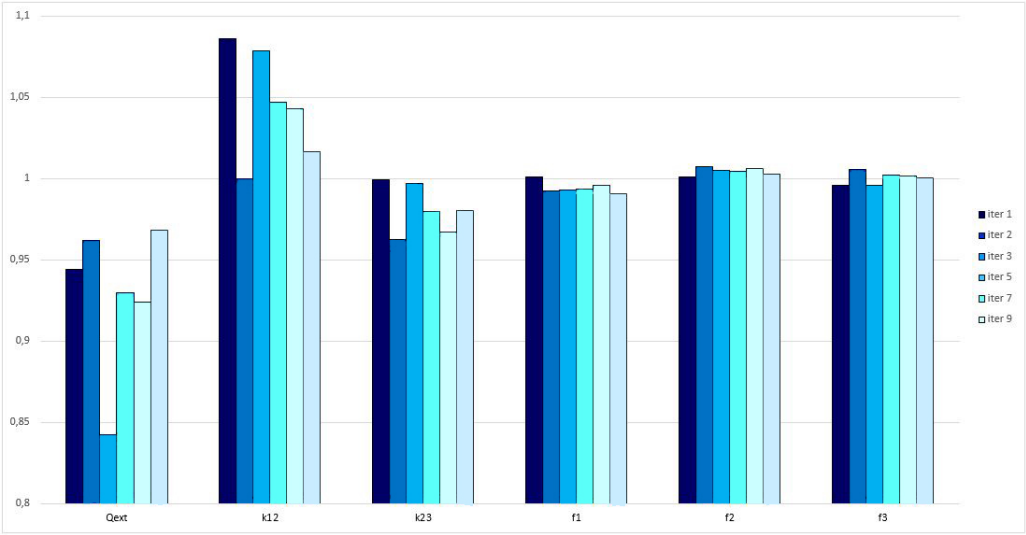

Figure 4.21: Evolution of Coarse Model Parameters Normalized to x_c^*.

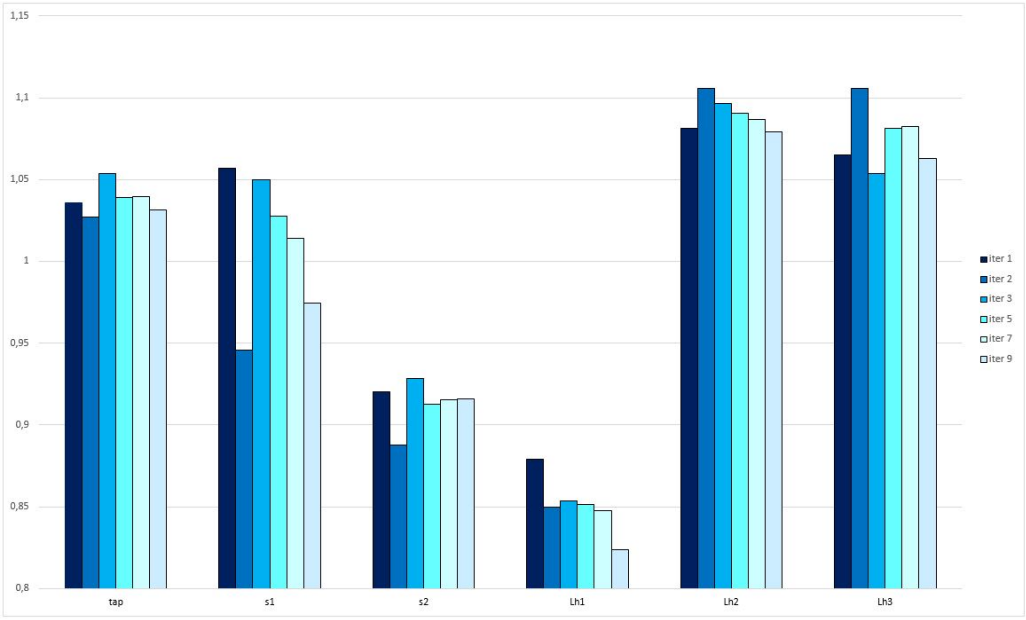

Figure 4.22: Evolution Fine Model Parameters Normalized to x_f^1.

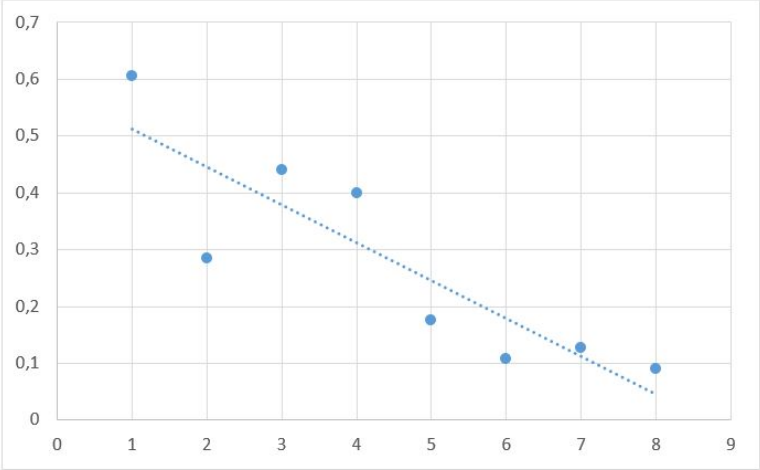

Figure 4.23: Evolution of Error.

And after applying all these iterations, we finally match our stopping criteria. The output is the following:

```
This is iteration: 9
Previous coarse model:
[5.267 ,0.1669,0.1199,1.9855,2.0078,2.004 ]
Fine model:
[14.2404621, 0.4563388, 0.7323776, 3.9071502, 5.0003245, 4.9783284]
New coarse model to match fine model:
[5.514  ,0.1642 ,0.1187 ,1.98787,2.01185,2.00473]
```

```
Previous h vector:
[ 0.0681033, 0.0104297, 0.0192057,-0.0470977,-0.0903655, 0.0245627]
New h vector:
[-0.0614264,-0.0039442,-0.0058693, 0.0115704, 0.0707088,-0.0157809]
Matrix B:
[[ 3.5366167, 0.374561 , 0.2454484,-0.0173333,-0.6303468,-1.1362712],
 [-0.019537 ,-0.1667146,-0.0061607,-0.0255431, 0.023199 , 0.0341318],
 [-0.0052491,-0.0024041,-0.0808161,-0.0102684, 0.0099822, 0.0122474],
 [ 0.0375729,-0.0000764,-0.0033727,-0.0951423, 0.0209277, 0.0292165],
 [-0.0051735, 0.0032011, 0.0047435, 0.0247826,-0.0697118,-0.0199719],
 [ 0.0088343, 0.007542 , 0.0078357, 0.0478482,-0.0314866,-0.098927 ]]
New fine model:
[14.1790357, 0.4523946, 0.7265083, 3.9187206, 5.0710333, 4.9625475]
Error:
0.09594713769542024
```

And as it can be observed in the output of the script, the "error", which in this case is the modulus of the variation vector h, is less than 0.1, which was our aim, because that means that the changes in our physical dimensions are not that significant any more and we can stop the algorithm. Finally, the frequency response of the obtained filter is plotted.

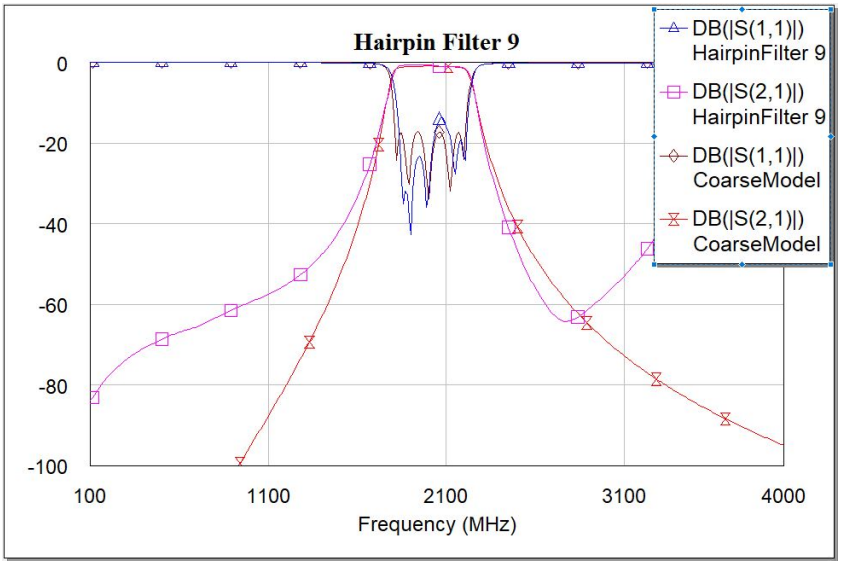

Figure 4.24: Optimized Frequency Response.

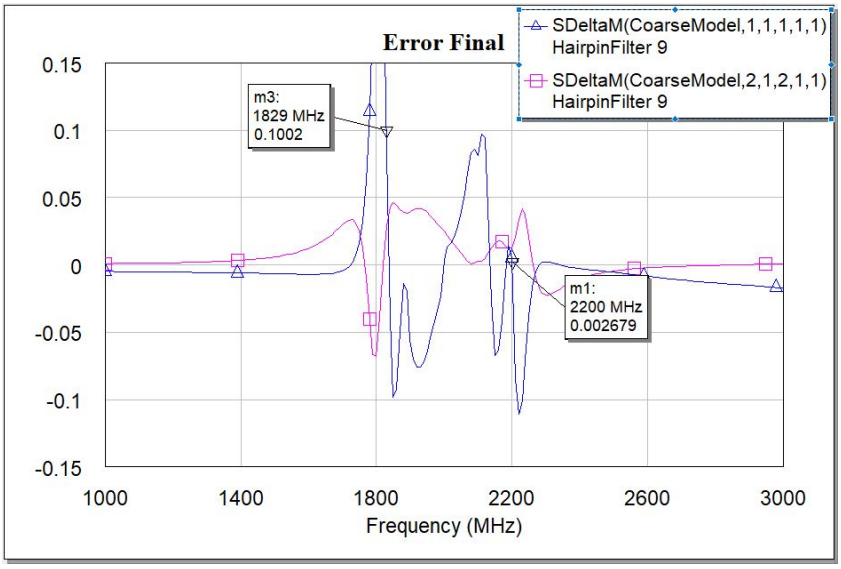

Figure 4.25: Final Freq. Response vs Ideal.

It can be appreciated in Fig. 4.25 that the filter presents a frequency response with an error lower to 10% compared to the ideal frequency response, in almost the complete pass band.

Filter FOM			
S_{11} (dB)	S_{21} (dB)	f_{c1} (GHz)	f_{c2} (GHz)
-13.64	-0.99	1.79	2.15

Table 4.6: Final Filter Design Specs.

The final dimensions and layout for our hairpin filter are the following:

Initial Fine Model Params					
t (mm)	s_1 (mm)	s_2 (mm)	L_{h1} (mm)	L_{h2} (mm)	L_{h3} (mm)
13.7	0.458	0.8	4.6	4.6	4.6
Final Fine Model Params					
t (mm)	s_1 (mm)	s_2 (mm)	L_{h1} (mm)	L_{h2} (mm)	L_{h3} (mm)
14.1583	0.43138	0.70625	4.00075	5.12098	4.96309

Table 4.7: Final vs Initial Fine Model Parameters.

In Fig. 4.26, we can see the final layout implemented with all the dimensions in mm.

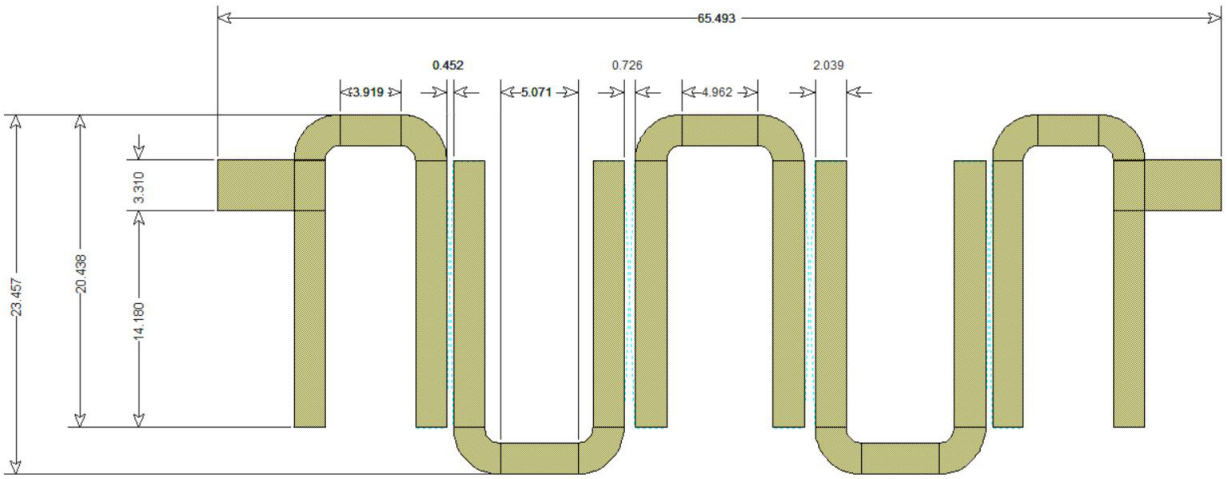

Figure 4.26: Optimized Final Layout.

Chapter 5

Design Example 2: Open Loop Filter

5.1 Introduction

Step by step, we have successfully designed our first hairpin filter from Chap. 4. But it is time to go a little bit deeper and try a more complex design as it was stated at the very beginning of this report. This time, an open loop resonator-based filter will be implemented. The main difference with the other design, is that in this case, the resonators are $\frac{\lambda}{2}$ resonators bent into squares, which compacts them a lot and reduces the area of the filter considerably, but also introduces cross-couplings between non-adjacent resonators, which in the frequency response, turns out to be transmission zeros. Understanding this theoretical concept about this filter, we can move to its design process.

5.2 Theoretical design

As in the previous example, we can distinguish here between two different theoretical parts, the coarse model or circuital one and the fine model or microstrip one. But in this occasion, we have already computed the theoretical values for the microstrip lines, since we are going to use $\frac{\lambda}{2}$ resonators again. Regarding the circuital part, we are going to tackle the design from a different perspective this time.

5.2.1 Microstrip theoretical calculations

Re-using the previously calculated values in Chap. 4, we have:

Microstrip Lines values for Substrate = RO 4003-C						
ϵ_r	H (mm)	W(mm)	Z_c (Ω)	W_0(mm)	Z_0 (Ω)	L_{tot} (mm)
3.55	1.51	2.039	66.7	3.31	50	46.5

Table 5.1: Theoretical values for Microstrip Lines.

5.2.2 Circuital theoretical design

In the previous Hairpin filter, we followed an example from [1], but for this one, we are just going to fix the same filter specifications and carry out our design using optimization, but pursuing a pseudo-elliptical response this time, since our filter introduces zero in transmission.

Specs			
n	f0	FBW	Ripple
5	2 GHz	0.2	0.1 dB

Table 5.2: Specifications for the Open Loop filter design.

So, since we are going to approach our design by optimization, we will start by building our filter schematic.

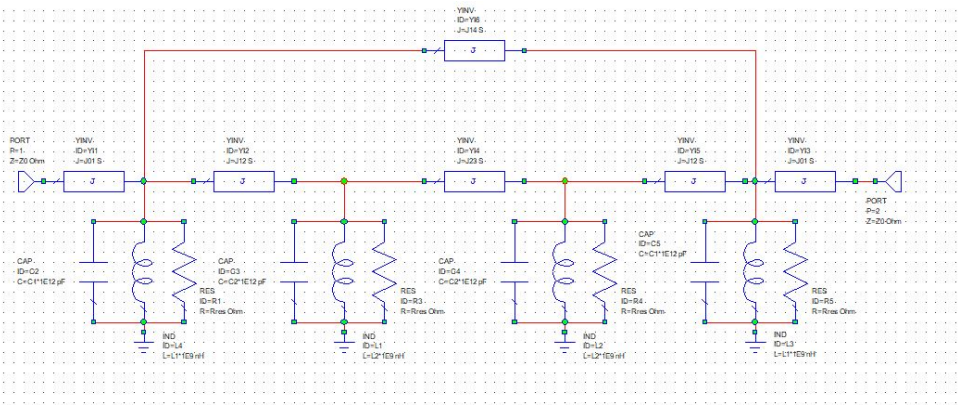

Figure 5.1: Coarse Model Schematic.

Having this ready, we are going to apply the same design technique as we did before, we will fix the value of C_{res} which translates into fixing the slope parameter of our filter. By applying optimization, we will let the AWR software optimize f_1, f_2, J_{01}, J_{12}, J_{23} and J_{14}.

Our very last step before starting optimizing our design, is to set up the optimization goals, which, taking into account that our design includes zeros in the transmission band, we are going to set the rejection bands at $f_0 \pm (1.2 \cdot f_c - f_c)$. In the following table we can see all the optimization rules or goals.

	$S_{1,1}$(dB)	$S_{2,1}$(dB)
1.8, 2.2 GHz	-	3
1.3 - 1.65 GHz	-	$<$ -40
2.4 - 2.7 GHz	-	$<$ -40
1.83 - 2.17 GHz	-	$>$ -0.8
1.817 - 2.187 GHz	$<$ - 13	-

Table 5.3: Optimization Goals.

And after some iterations, we obtain our ideal model, whose frequency response looks like:

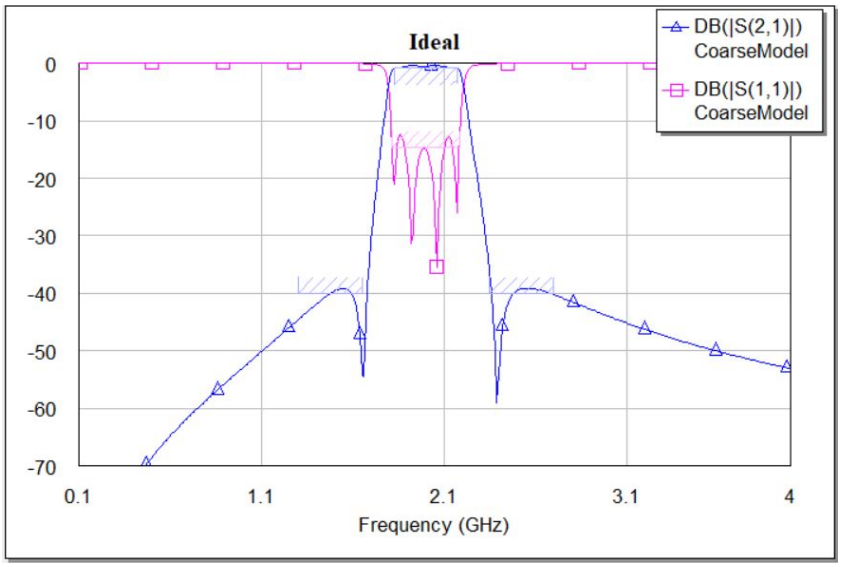

Figure 5.2: Pseudo-Elliptical Bandpass Ideal Frequency Response with Zero in Transmission.

Which is characterized by the following component values:

Ideal Model Params						
J_{01}	J_{12}	J_{23}	J_{14}	$R_{res}(\Omega)$	$C_{res}(pF)$	$L_{res}(nH)$
0.008985	0.003217	0.002991	-0.0004584	$1.18 \cdot 10^4$	1.89	3.384

Table 5.4: Theoretical values.

As it can be clearly observed in Fig. 5.2, the frequency response presents fours poles, and two transmission zeros.

Filter Specifications					
S_{11} (dB)	S_{21} (dB)	f_{c1} (GHz)	f_{c2} (GHz)	f_{rejec_1} (GHz)	f_{rejec_2} (GHz)
-12.5	-0.5	1.8	2.199	1.67	2.36

Table 5.5: Ideal Filter Design Specs.

Now that we have finished the optimization of our initial ideal model, we can compute the rest of the values that we will need to apply ASM.

$$Q_{ext} = \frac{w_0 C_{res}}{Z_0 J_{01}^2}, \qquad k_{i,i+1} = \frac{J_{i,i+1}}{w_0 C_{res}} \tag{5.1}$$

Applying the equations in 5.1, we obtain all the values that we need for our ASM algorithm.

Coarse Model Parameters					
Q_{ext}	k_{12}	k_{23}	k_{34}	f_1 (GHz)	f_2 (GHz)
7.35	0.1355	0.126	-0.0193	1.99	1.99

Table 5.6: Ideal Filter Design Coarse Parameters x_c^*.

And now we can move on to the next step, applying segmentation.

5.3 Segmentation process

For this filter, we are going to be using the previously stated parameters for ASM. Since we have four resonators, which translates into two frequencies f_1 and f_2, external quality factor Q_{ext}, two normal coupling coefficients k_{12}, k_{23} and the cross coupling coefficient k_{14}, which sum up to six parameters in total, and also are the main frequency response modifiers as well. Converted to the fine model, these parameters represent the tapping t or entry point into the filter, the lengths of the hairpin resonators L, and the physical separation between them s_1, s_2 and s_3. So, with everything set up, we can proceed, apply segmentation and start analyzing our fine model part by part.

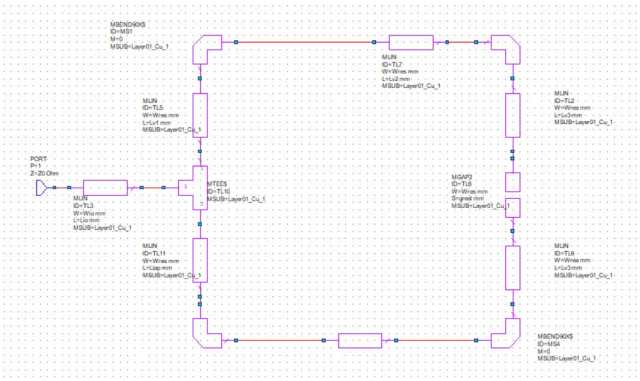

Figure 5.3: OpenLoop Resonator Schematic.

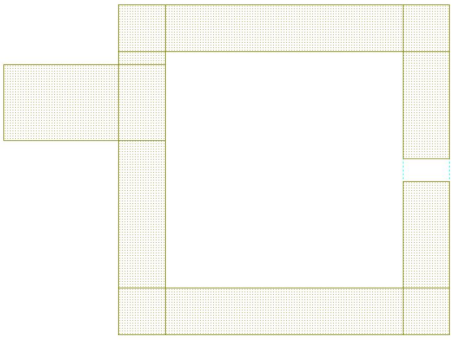

Figure 5.4: OpenLoop Resonator Layout.

The schematic has been designed with the help of AWR's components MLIN, MBEND90X$, MTEE$ and MGAP2. The total length of the resonator can be computed as:

$$L_{tot_{eff}} = L_{tot_0} + gap \tag{5.2}$$

The reason why we are applying Eq. 5.2 is because, in order to vary the resonator frequency, we need to change its total length. In the previous Hairpin design, this was quite easy, because by modifying the central length of the resonator, we could modify the frequency as well without affecting the rest of the parameters in a notorious way. But in this design, if we change the total length of the resonator, we are not only affecting its frequency but also the coupling coefficients with the rest of the resonators. As a result of this, in order to be able to tune each resonator frequency trying to minimize the effect caused on the rest of the parameters, it was decided to approach this task by modifying the gap g of each resonator.

So first of all, we are going to apply the same technique as we did in the previous design and we will center the resonator at 2 GHz, which leads us to a final total length of : $L_{tot} = 40.6$ mm. We will fix this length, and from there on, we will modify the resonator total length by increasing or decreasing its gap g.

This was our last step before starting our parameter extraction. Using the same graphs and equations as in the previous design of Chap. 4, we can obtain all the necessary curves to initialize our ASM algorithm one more time.

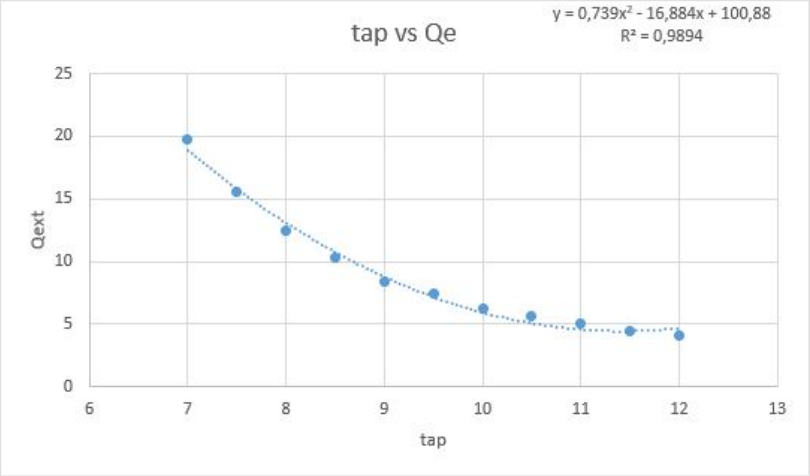

Figure 5.5: Tapping t vs Q_{ext} characteristic curve.

From this graph, and in order to obtain our theoretically calculated Q_{ext} of 7.35, we need to fix an initial tapping t of 9.44 mm. Then, we are going to analyze the frequency variation with the resonator length. In this case, as it was specified previously, this variation will be performed over gap g.

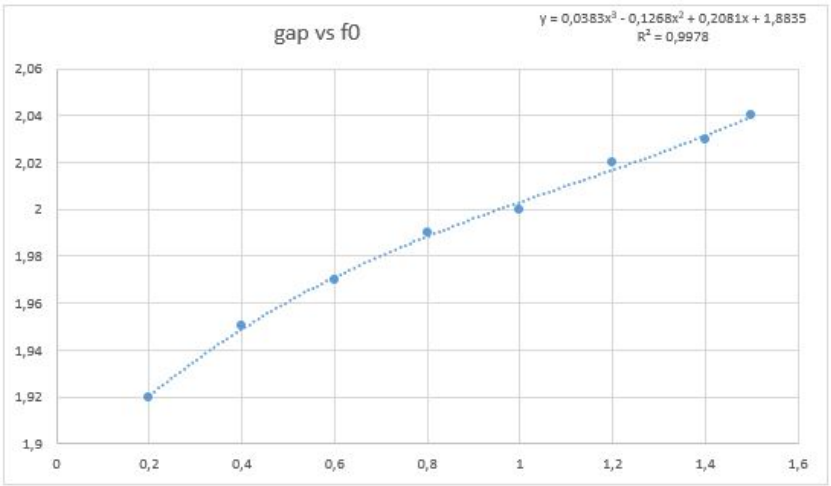

Figure 5.6: f_0 vs *gapg* characteristic curve.

For our initial value of $f_0 = 2$ GHz, we must set all gap values g_1 and g_2 at 0.75 mm.

Finally, we will obtain the curve for k_{ij} coefficients in terms of the physical separation s. But this design is going to be a little bit different than our previous example. Since we have three different situations of coupling, based on the type, electric or magnetic, and based in the orientation of the

open loop resonators themselves, we are going to analyze and characterize all these cases.

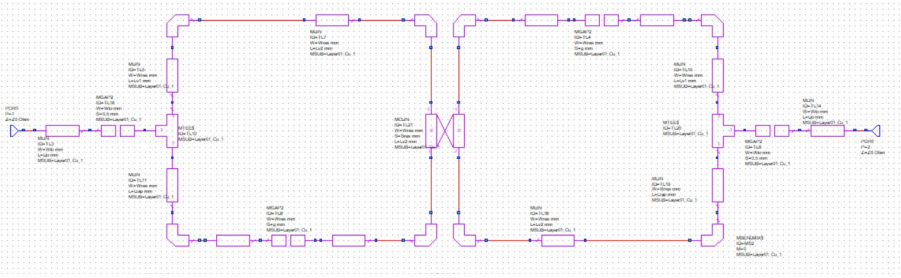

Figure 5.7: Schematic for measuring gap vs k_{ij} curve.

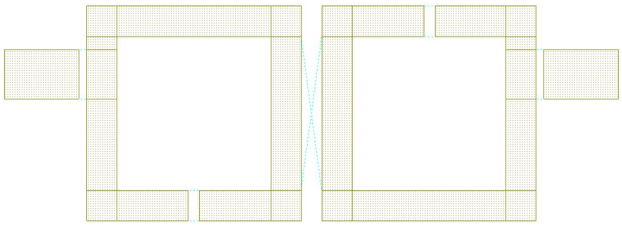

Figure 5.8: Schematic Layout.

The obtained curve is the following.

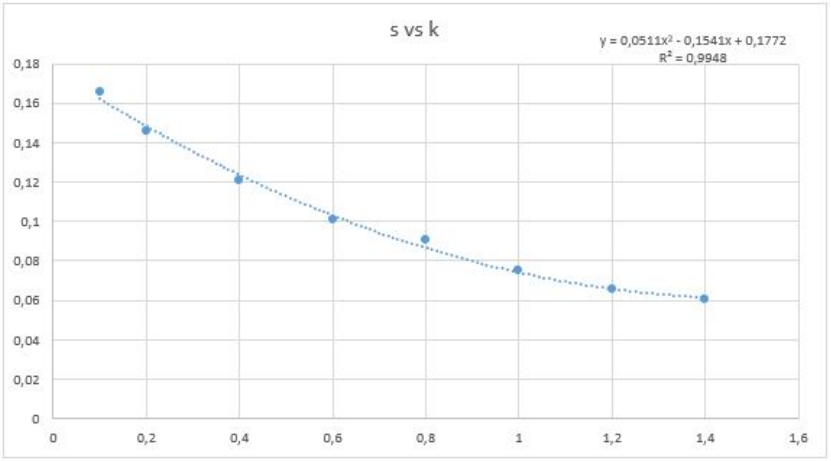

Figure 5.9: S vs k_{ij} characteristic curve type 1.

For the theoretical $k_{12} = k_{34}$ value of 0.1355, the separation s_1 is 0.3 mm.

The next magnetic coupling type can be observed in Figs. 5.10 and 5.11.

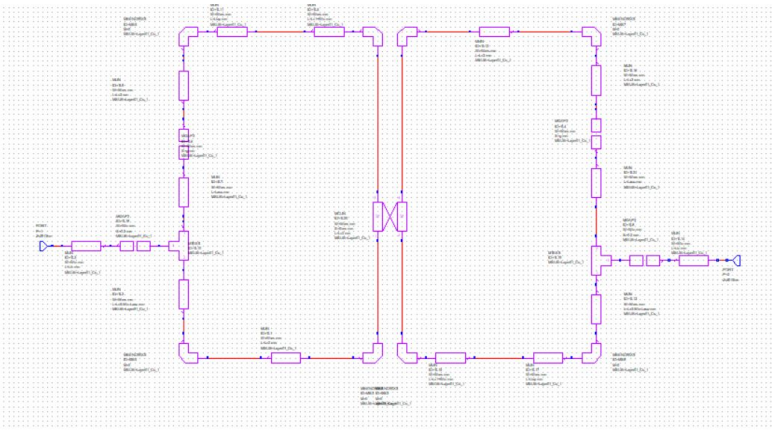

Figure 5.10: Schematic for measuring gap vs k_{ij} curve.

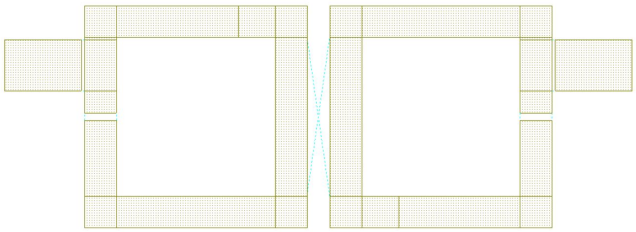

Figure 5.11: Schematic Layout.

Whose characteristic figure can be observed in Fig. 5.12

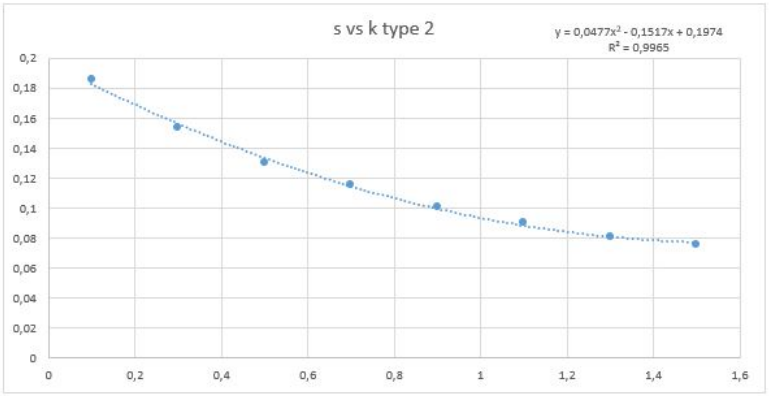

Figure 5.12: s vs k_{ij} characteristic curve type 2.

For our k_{23} value of 0.123, the separation s_2 is 0.55 mm.

Finally, we are going to analyze the electric coupling.

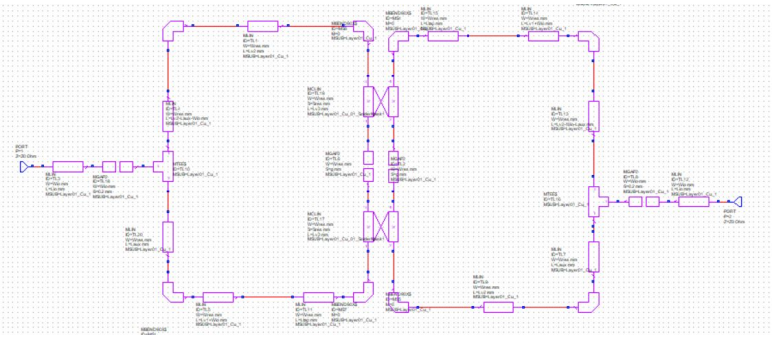

Figure 5.13: Electric Coupling Schematic.

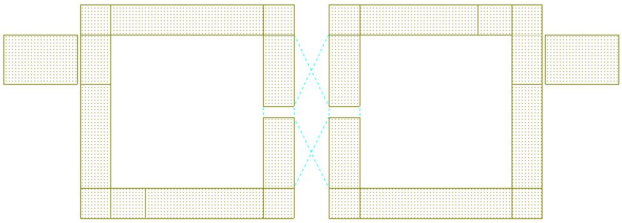

Figure 5.14: Schematic Layout.

Whose characteristic figure can be observed in Fig. 5.15

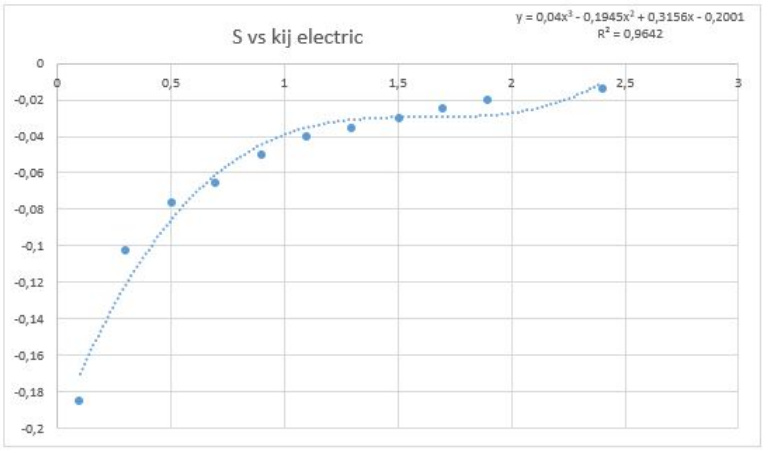

Figure 5.15: s vs k_{ij} characteristic curve for electric coupling.

From the previous curve, and for the theoretically calculated value of $k_{14} = -0.0193$, we obtain an initial separation value of: $s_3 = 2.2$ mm.

And with this steps completed, we are ready now to set up our first fine model approach and start applying ASM.

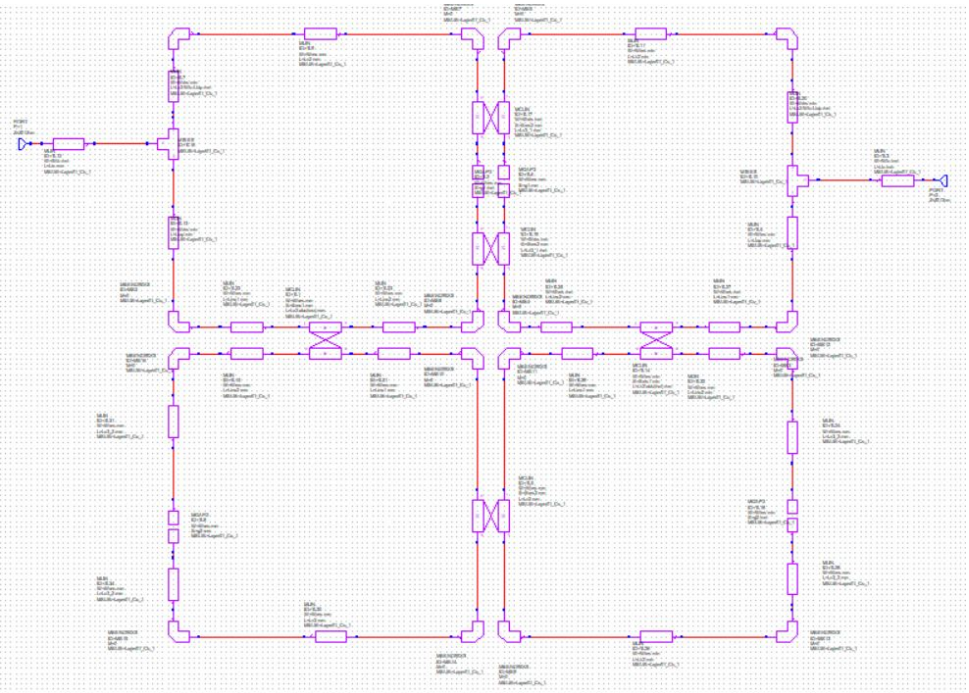

Figure 5.16: Fine Model First Approach Schematic.

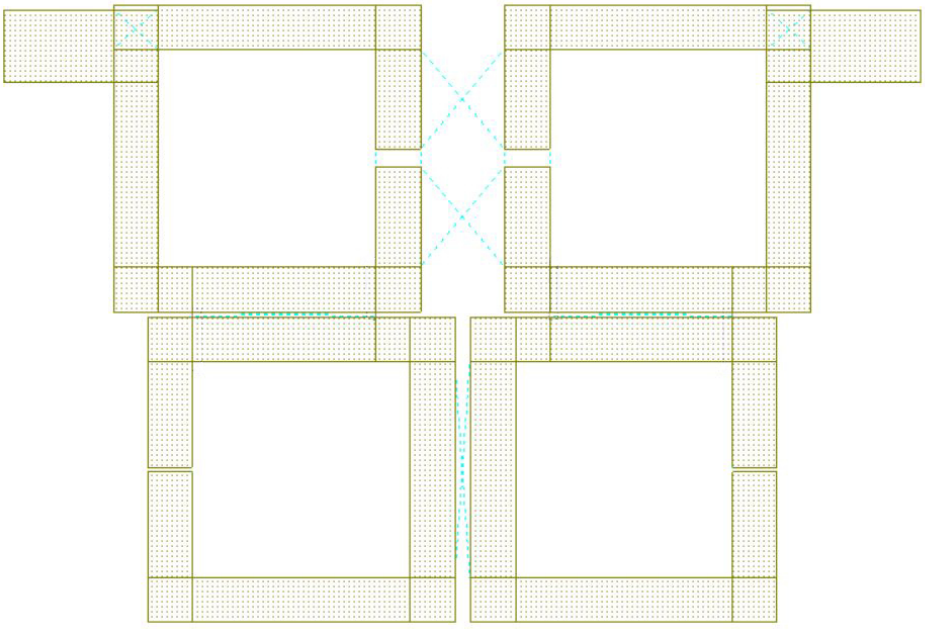

Figure 5.17: Fine Model First Approach Schematic Layout.

After building the final schematic, the frequency of the filter was shifted down to be re-centered at 2 GHz, so the total length of the resonators was slightly decreased to 39 mm.

After all these adjustments, the obtained frequency response can be observed in Fig. 5.18

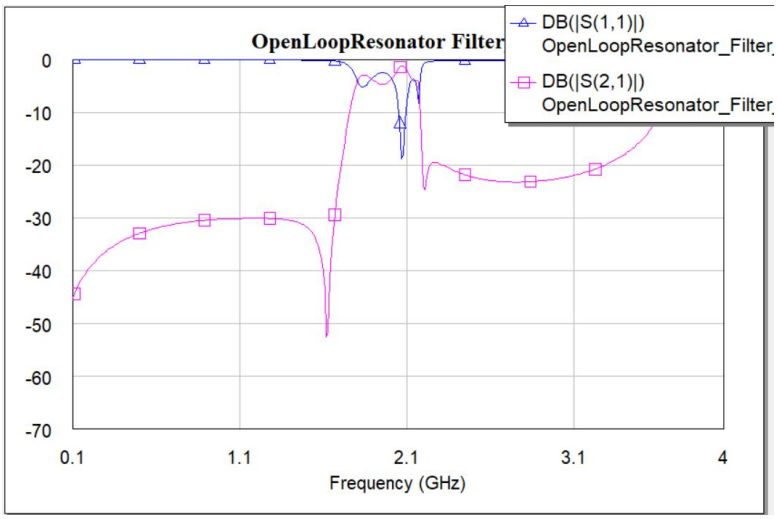

Figure 5.18: Initial Fine Model EM Simulation.

5.4 ASM Optimization

In our previous design, it was decided to use an stopping criteria based on the variation vector h computed by the ASM algorithm, since that means the modifications that the algorithm is applying over the previous model are not significant any more, but for this design, we are going to follow the alternative criteria, which, as it was previously defined, compares the resulting frequency response from each iteration with the ideal frequency response, and if the error is lower than an established threshold, then we can stop applying the algorithm.

The reason why it was decided to follow this criteria for this design is because this topology is more delicate, and it may happen that even if ASM correctly approaches the desired response, it could oscillate and never converge.

So now, following the same procedure as we did in Chap. 4, our task is to build the Broyden matrix B, but first, we need to compute the value of the partial derivatives at the initial point.

$$Q(t) = 1.478x - 16.884, \qquad \left.\frac{\partial Q}{\partial t}\right|_{t=9.75mm} = -2.4735 \tag{5.3}$$

$$k_{12}(s) = 0.1022x - 0.1541, \qquad \left.\frac{\partial k_{12}}{\partial s}\right|_{s_1=0.2} = -0.13356 \tag{5.4}$$

$$k_{23}(s) = 0.0954x - 0.1517, \qquad \left.\frac{\partial k_{23}}{\partial s}\right|_{s_2=0.55} = -0.099 \tag{5.5}$$

$$k_{14}(s) = 0.1022x - 0.1541, \qquad \left.\frac{\partial k_{14}}{\partial s}\right|_{s_3=2.2} = 0.0384 \tag{5.6}$$

$$f(g) = 0.115x^2 - 0.2536x + 0.208, \qquad \left.\frac{\partial f}{\partial g}\right|_{g_{1,2}=0.75} = 0.0825 \tag{5.7}$$

Once we have completed these calculations, we can build our Broyden matrix B, which is going to be a 6x6 matrix again.

$$B = \begin{bmatrix} -2.4735 & 0 & 0 & 0 & 0 & 0 \\ 0 & -0.13356 & 0 & 0 & 0 & 0 \\ 0 & 0 & -0.099 & 0 & 0 & 0 \\ 0 & 0 & 0 & 0.0384 & 0 & 0 \\ 0 & 0 & 0 & 0 & 0.0825 & 0 \\ 0 & 0 & 0 & 0 & 0 & 0.0825 \end{bmatrix} \tag{5.8}$$

Now, we have everything ready to start running the ASM algorithm. But in this design, the obtained initial point from applying segmentation is not really that good, and since the design is a bit more complex, it is not a good enough starting model to ensure that ASM optimization algorithm will converge properly.

So, since we obtained the ideal model of this filter applying optimization, we are going to follow the same approach and apply some optimization to our initial model. This will improve the starting point a little bit and then finally, we can start applying ASM optimization.

After some iterations, the optimizer provides us some new dimensions whose frequency response has been improved.

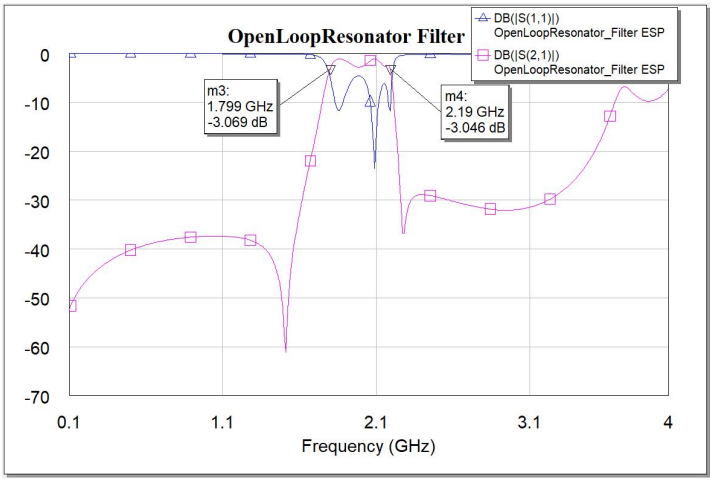

Figure 5.19: Optimized Initial Fine Model Freq. Response.

Even though it may seem like the change does not really make a big difference, due to the delicate nature of the filter and of the ASM techniques themselves, just a simple change like this one, can turn out to be something crucial for the final convergence of the design.

The final dimensions of the initial point are described in Tab. 5.7.

Coarse Model Parameters					
$tap\ (mm)$	$s_1\ (mm)$	$s_2\ (mm)$	$s_3\ (mm)$	$g_1\ (mm)$	$g_2\ (mm)$
9.7	0.29	0.4548	3.8	1.325	0.7345

Table 5.7: Initial Fine Model After Optimization.

These variations does not suppose a huge change or impact over the previously computed ASM parameters, so we can just proceed and follow the same procedure as we did before with Hairpin resonators based filter.

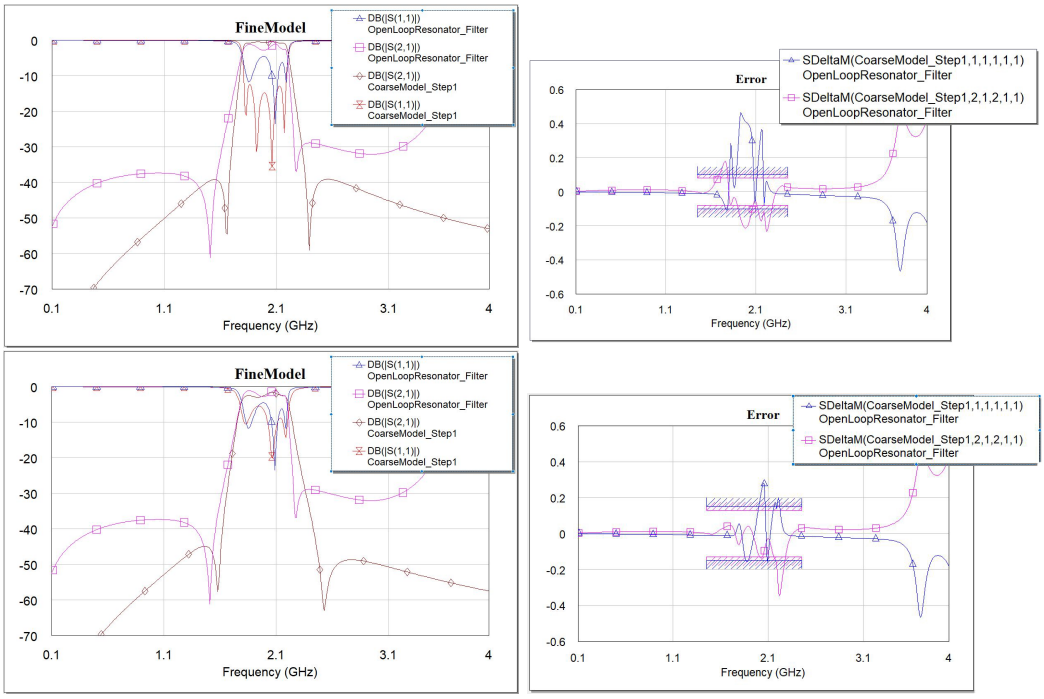

Figure 5.20: Fine Model vs Coarse Model PE in Iteration 1.

It should be noted that, even though the error might see like being too high, by taking a look at the frequency response comparison graph, it can be appreciated that the effective band is quite similar, being most of the error on the outside rejection bands.

After applying PE, we go ahead and compute the next fine model, perform an EM simulation, and surprisingly, the obtained frequency response was the following:

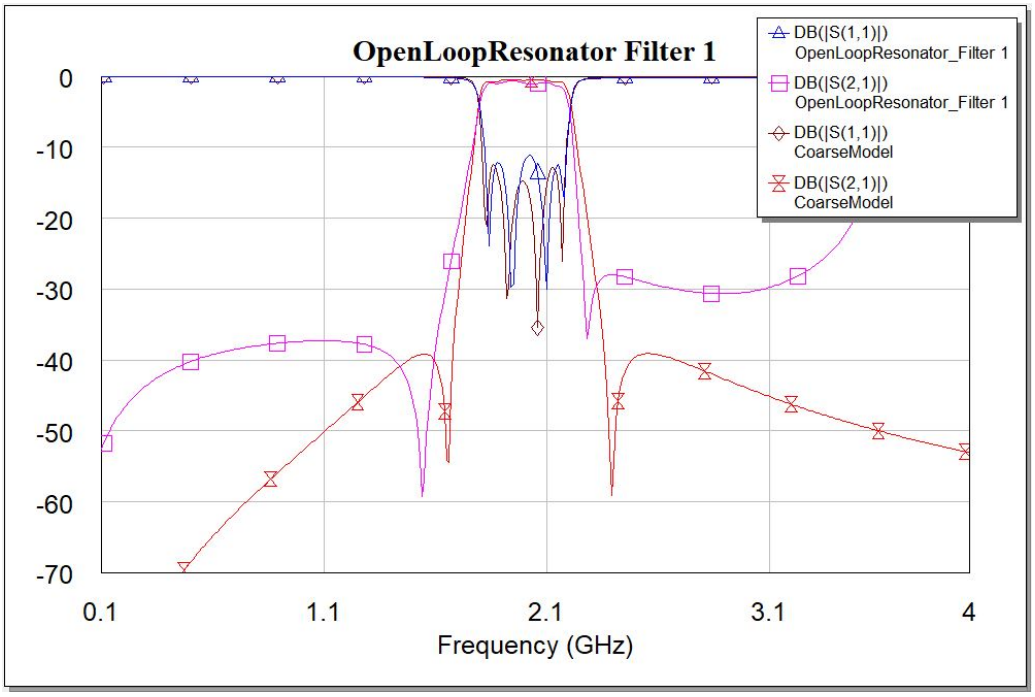

Figure 5.21: Iteration 1 Fine Model Freq. Response.

Which has an error lower than 15% in the useful band ≈ 1.8 - 2.2 GHz, and which is the threshold we fixed for this second design, since it is more complex.

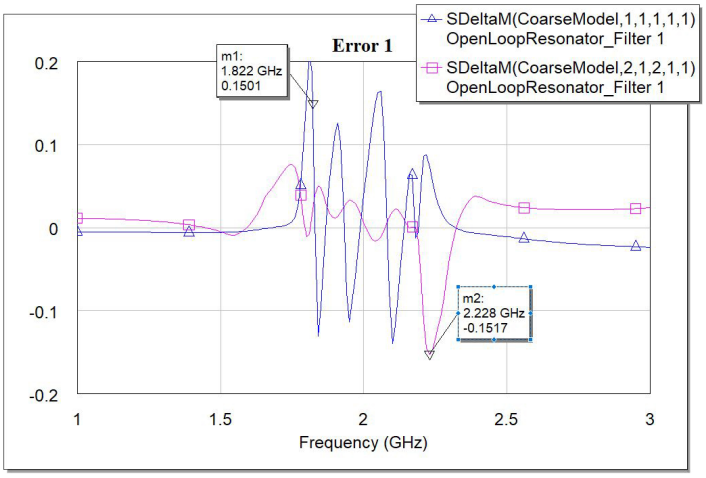

Figure 5.22: Final Filter Model Error

Which presents a frequency response evolution of the following form.

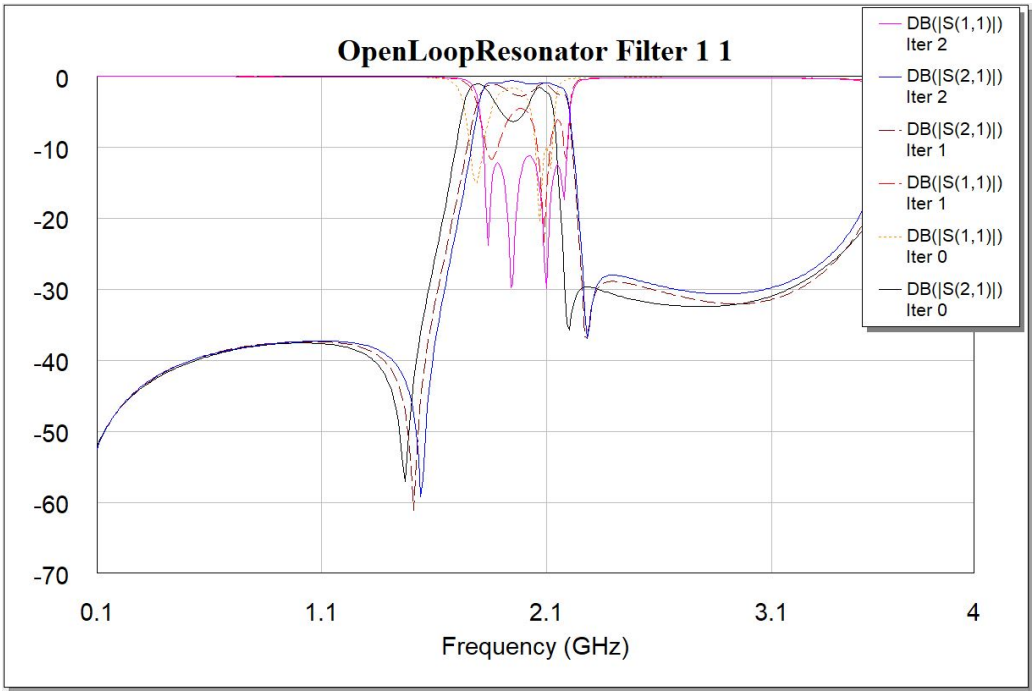

Figure 5.23: Evolution of Frequency Response trough Iterations.

Briefly going over the evolution of the different parameters through the iterations, we can have a look at it in the graphs below.

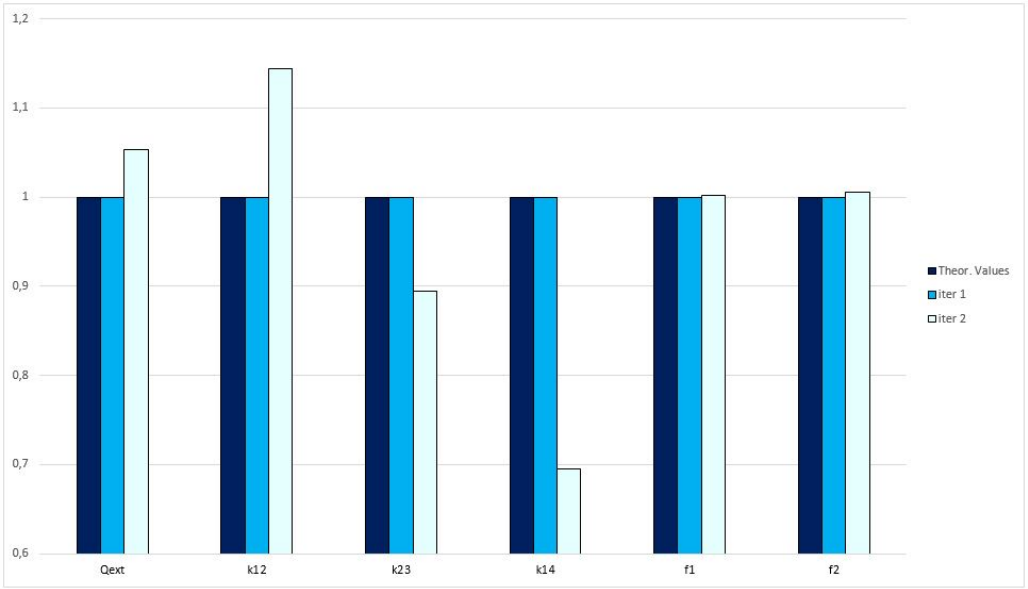

Figure 5.24: Evolution of the Coarse Model Params with each Iteration and normalized to initial values xc_0.

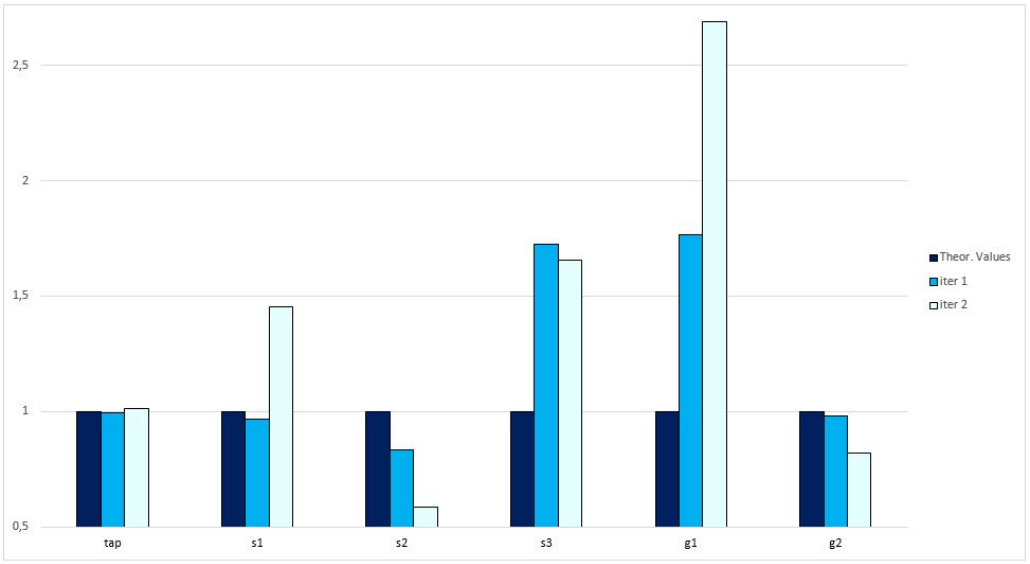

Figure 5.25: Evolution of the Fine Model Params with each Iteration and normalized to initial values xf_0.

Filter FOM			
S_{11} (dB)	S_{21} (dB)	f_{c1} (GHz)	f_{c2} (GHz)
-11.2	-1.07	1.793	2.192

Table 5.8: Final Filter Design Specs.

The final dimensions and layout for our Open Loop filter are the following:

Initial Fine Model Params					
t (mm)	s_1 (mm)	s_2 (mm)	s_3 (mm)	g_1 (mm)	g_2 (mm)
9.75	0.3	0.55	2.2	0.75	0.75
Final Fine Model Params					
t (mm)	s_1 (mm)	s_2 (mm)	s_3 (mm)	g_1 (mm)	g_2 (mm
9.8576	0.436	0.321	3,646	2,016	0,61328

Table 5.9: Final vs Initial Fine Model Parameters.

And finall, in Fig. 5.26, we can see the final layout implemented with all the dimensions in mm.

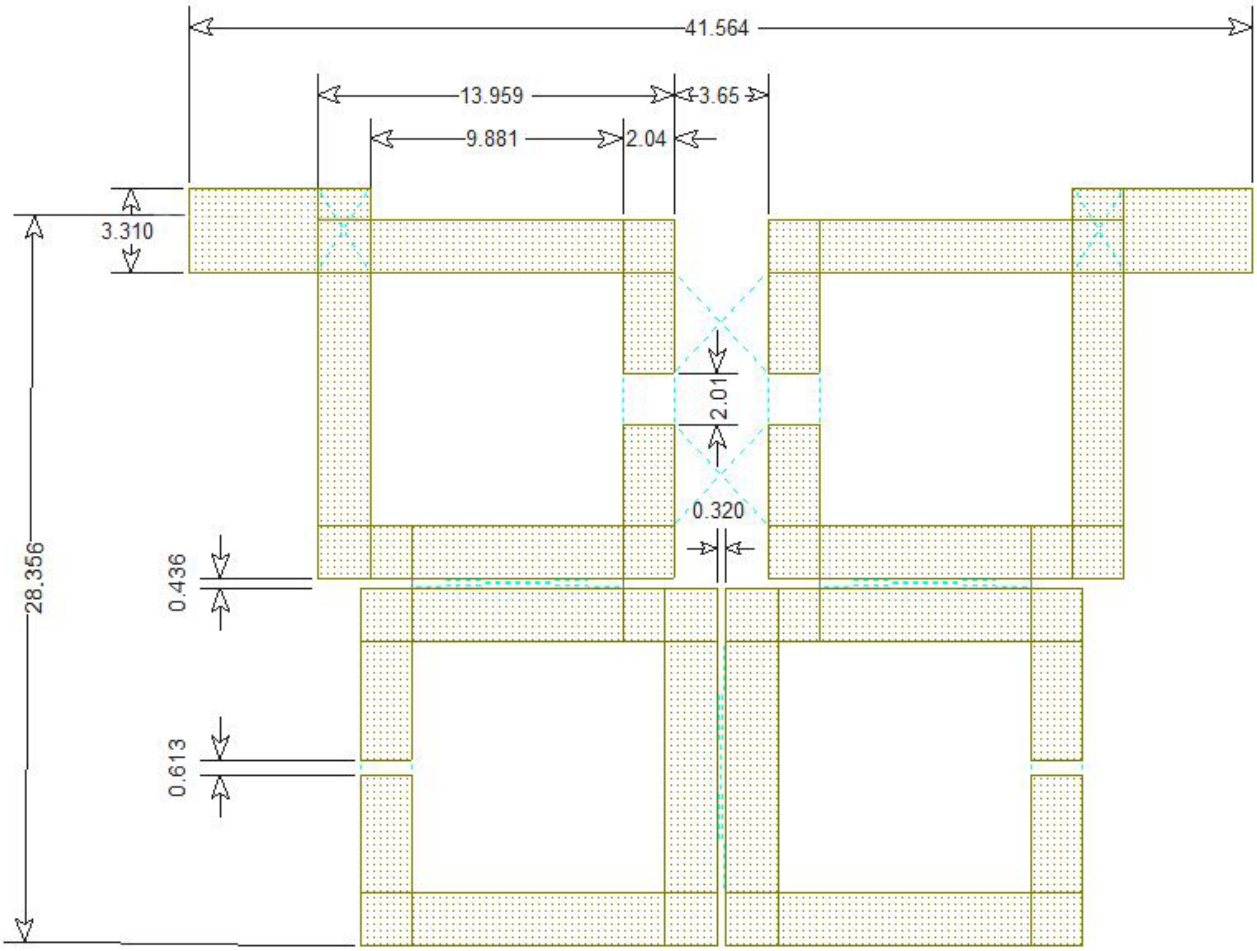

Figure 5.26: Optimized Final Layout.

Chapter 6

Conclusions and Future Lines of Research

6.1 Conclusions

First of all, I would like to thank the reader for arriving to what is going to be the very last episode of this report.

Having said this, and as a final conclusion, I would like to highlight the **simplicity** and **effectiveness** of the ASM techniques. It has been shown how, by applying a really straightforward procedure, we can get practical filters, which take a relatively short period of time to design thanks to the applied techniques, and whose frequency response is fairly enough approximated to the ideal one.

However, we must keep in mind that this technique is not bulletproof, and there may be certain designs, where the algorithm will not converge to our desired response, but we can for sure agree that whenever it converges, it is a really powerful tool in filter designing.

6.2 Future lines of research

As future lines of research, the algorithm could be tested in many other different ways, and in a lot of different designs and alternative topologies, and of course, check whether it would be viable to use as a default designing method for universities, research centers..

Nevertheless, for the incoming 5G revolution and this fast evolving world of telecommunications and technology in general, it would be truly interesting to refine an algorithm which allows us to design and manufacture our projects efficiently and faster than applying other approaches, because we would have a tool powerful enough to keep track of the latest applications which usually require a change or improvement on hardware.

Bibliography

[1] Jia-Sheng Hong, M. J. Lancaster, *Microstrip Filter for RF / Microwave Applications*. Second Edition, Wiley 2011.

[2] David M. Pozar, *Microwave Engineering*. Second edition, 1997.

[3] J. E. Rayas-Sanchez,*"Power in Simplicity with ASM: Tracing the Aggressive Space Mapping Algorithm Over Two Decades of Development and Engineering Applications,"* in IEEE Microwave Magazine, vol. 17, no. 4, pp. 64-76, April 2016

[4] J. W. Bandler, R. M. Biernacki, S. H. Chen, P. A. Grobelny, R. H. Hemmers,*"Space mapping technique for electromagnetic optimization"*. IEEE Trans. Microwave Theory Tech., vol. 42, no. 12, pp. 2536-2544, Dec. 1994.

[5] S. Koziel, Q. S. Cheng, J. W. Bandler,*"Space mapping"*. IEEE Microwave Mag., vol. 9, pp. 105-122, Dec. 2008.

[6] Rodriguez, Ana and Morro, Jose and Selga, Jordi and Sans, Marc and Ossorio, Javier and Guglielmi, Marco and Martin, Ferran and Boria, Vicente. *Robust optimization and tuning of microwave filters and artificial transmission lines using aggressive space mapping techniques.* 2017. 1501-1504. 10.1109/MWSYM.2017.8058909.

[7] Alhaddad, Mohammed.*"Band Pass Filter with Open Loop Resonator"*. 2015, 10.13140/RG.2.1.3081.4560.

[8] J. W. Bandler et al. *"Space mapping: the state of the art,"*. in IEEE Transactions on Microwave Theory and Techniques, vol. 52, no. 1, pp. 337-361, Jan. 2004.

[9] J. B. Ness, *"A unified approach to the design, measurement, and tuning of coupled-resonator filters,"* in IEEE Transactions on Microwave Theory and Techniques, vol. 46, no. 4, pp. 343-351, April 1998.

[10] J. W. Bandler, M. A. Ismail, J. E. Rayas-Sanchez, *"Expanded space mapping design framework exploiting preassigned parameters"*, pp. 1151-1154, 2001-May.

[11] P. W. Hemker, D. Echeverria, J. Comput. Phys.*"A trust-region strategy for manifold-mapping optimization",*, vol. 224, pp. 464-475, Apr. 2007.

[12] J. W. Bandler, R. M. Biernacki, S. H. Chen, *"Fully automated space mapping optimization of 3D structures"* , pp. 753-756, 1996-June.

[13] Chao Zhang, Feng Feng, Qi-Jun Zhang, John W. Bandler, *"Enhanced cognition-driven formulation of space mapping for equal-ripple optimisation of microwave filters"*. Microwaves Antennas and Propagation IET, vol. 12, no. 1, pp. 82-91, 2018.

[14] Nick Davis, *" An introduction to filters"* . July 2017. https://www.allaboutcircuits.com/technical-articles/an-introduction-to-filters/

[15] Wikipedia contributors In Wikipedia, The Free Encyclopedia, *Electronic filter*. September 2019. https://en.wikipedia.org/w/index.php?title=Electronic_filter&oldid=914643253